UNIVERSITÀ DEGLI STUDI DI PARMA
Dottorato di Ricerca in Fisica
Ciclo XXV

Correlators of Wilson loops on Hopf fibrations

in the AdS_5/CFT_4 correspondence

Coordinatore:
Chiar.mo Prof. PIERPAOLO LOTTICI

Supervisore:
Dott. LUCA GRIGUOLO

Dottorando:
STEFANO MORI

Anno Accademico 2012/2013

ויאמר אלהים יהי אור ויהי אור

בראשׁיה 1:3

Io stimo più il trovar un vero, benché di cosa leggiera,
che 'l disputar lungamente delle massime questioni
senza conseguir verità nissuna.
(Galileo Galilei, *Scritti letterari*)

Contents

1 The correspondence and its observables **1**

1.1 AdS_5/CFT_4 correspondence 1

1.1.1 $\mathcal{N} = 4$ SYM 1

1.1.2 AdS space 2

1.2 Brane construction 4

1.3 Symmetries matching 6

1.4 AdS/CFT dictionary 7

1.5 Integrability 9

1.6 Wilson loops and Minimal surfaces 10

1.7 Mixed correlation functions and local operator insertion . . . 13

1.8 Main results from the correspondence 14

2 Wilson Loops and Supersymmetry **17**

2.1 BPS configurations 17

2.2 Zarembo supersymmetric loops 18

2.3 DGRT loops 20

2.3.1 Hopf fibers 23

2.4 Matrix model 25

2.5 Calibrated surfaces 27

3 Strong coupling results **31**

3.1 Basic examples 31

3.1.1 Straight line 31

3.1.2 Cirle 32

3.1.3 Antiparallel lines 33

3.1.4 1/4 BPS circular loop 33

3.2 Systematic regularization 35

3.3 Ansatz and excited charges 36

3.4 Hints of 1-loop computation 37

4 Hopf fibers correlators **41**
4.1 Strong coupling solution 41
4.1.1 S^5 motion 42
4.1.2 AdS_5 motion 43
4.1.3 Boundary conditions 45
4.1.4 Solutions to the equations of motion 45
4.2 Discussion of results 46
4.2.1 Coincident circles with different scalar couplings . . . 46
4.2.2 Coplanar loops of different radii 47
4.2.3 Fibers with equal radius and scalar coupling 49
4.2.4 Fibers with equal radius and different scalar couplings 51
4.2.5 Fibers with different radii 54
4.2.6 Coplanar fibers with different radii and scalar couplings 54
4.2.7 General case 54
4.3 Weak coupling 57
4.4 Static potential 58
4.5 Hints of 3-point functions 62

5 Conclusions **63**

A Superalgebra **67**

B Dirac matrices **69**

C Elliptic Functions **71**

D Details of strong coupling correlator **73**

Chapter 1

The correspondence and its observables

1.1. AdS_5/CFT_4 correspondence

AdS_5/SYM_4 is the most studied case of gauge/gravity duality. It is the first attempt to make quantitative predictions through holography.

The 4-dimensional field theory is the $\mathcal{N} = 4$ maximally supersymmetric Yang-Mills theory (SYM) with gauge symmetry $SU(N)$. The theory is interacting and has vanishing β-function. It represents the first example of non-trivial conformal theory in more than two dimensions. The Maldacena conjecture [1] states that it is equivalent (in the planar limit $N \to \infty$) to the type IIB superstring theory on the curved background $AdS_5 \times S^5$.

The equivalence can be argued by noting that the conformal group in four dimensions $SO(2,4)$ is the group of isometries of 5 dimensional AdS. The conjecture has then been made quantitative by building a precise dictionary between observables in the two theories. In particular, the correlation functions of dual operators on both sides of the correspondence can be computed. Recently, the problem of computing two points functions was solved by integrability techniques [2] and the three-point functions are under investigation, with the hope that planar $\mathcal{N} = 4$ SYM can be exactly solved by these methods.

1.1.1. $\mathcal{N} = 4$ SYM

The $\mathcal{N} = 4$ supermultiplet in four dimensions is the maximally supersymmetric multiplet that can be built, if we restrict the fields to have spin at most one. It contains a vector field A_μ, four spinor in the **4** of $SU(4)$ and six real scalar transforming in the **6** of $SO(6) \simeq SU(4)$. All the fields take value in the adjoint representation of the gauge group $SU(N)$.

The $\mathcal{N} = 4$ SYM action on $\mathbb{R}^4$ is completely fixed by the symmetry and

is given by [3]

$$S = \frac{1}{g^2}\int \mathrm{d}^4x\, \mathrm{Tr}\Big(\frac{1}{2}F_{\mu\nu}^2 + (D_\mu\Phi_I)^2 - \frac{1}{2}\sum_{I,J}[\Phi_I,\Phi_J]^2 + \\ + \bar\Psi^a\Gamma^\mu D_\mu\Psi_a + i\Psi_a\Gamma^{Iab}[\Phi_I,\Psi_b] + i\bar\Psi^a\Gamma^I_{ab}[\Phi_I,\bar\Psi^b]\Big)\,.$$

where $\mu,\nu = 1,\dots,4$ are the space-time indices, $a,b = 1,\dots,4$ are the indices of the **4** and $I = 1,\dots,6$ are the indices of the **6** representations of $SU(4)_R$ R-symmetry. $D = \mathrm{d} + A$ is the covariant derivative, with curvature $F_{\mu\nu} = [D_\mu, D_\nu]$.

The only free parameters of the theory are the coupling constant g_{YM} and the number of colors N.

For the purpose of this work, only the first two terms will be taken into account, since at the lower level in perturbation theory only the gauge field and the scalars are contributing. However, to consider higher level of perturbation theory, fermions and 4-scalar interactions must be taken into account and the computation becomes much more involved.

One striking feature of this theory is the vanishing of its β-function: this means that the theory is still conformal at quantum level, thus the $SO(2,4)$ conformal is not broken by renormalization.

Moreover, in the large N limit, the theory further simplifies. If we take $N \to \infty$ while keeping $\lambda = g^2_{\mathrm{YM}}N$ fixed, the Feynman diagrams organize themselves in a topological expansion in powers of $1/N$ and at the leading order only planar diagrams contribute [4].

1.1.2. AdS space

In order to set the notation, we will briefly describe the AdS space in the coordinate systems that will be used in the following.

The first coordinates system, known as Poincaré patch, enlights the structure of the conformal boundary of AdS. In this system, AdS space is described by (y, x^μ), with the metric

$$g_{mn} = \frac{1}{y^2}\mathrm{diag}\,[\,1, g_{\mu\nu}\,]\,.$$

The boundary is at $y = 0$ and it is isomorphic to Minkowski or Euclidean plane, depending on the initial choice for the signature for the AdS metric: if we start from Lorentzian (resp. Euclidean) signature, the boundary is Minkowski (resp. Euclidean) flat space.

The second coordinates system, that we will mostly use in explicit computations, is known as global coordinates patch. We will choose the coordinates tailored to the Hopf fibration that we will study in chapter 4. We

describe AdS_5 with the metric

$$g_{\mu\nu} = \begin{pmatrix} 1 & & \\ & \cosh^2\rho & \\ & & \sinh^2\rho\; g_{ij}^{\mathrm{Hopf}} \end{pmatrix} \tag{1.1}$$

where g_{ij}^{Hopf} is the metric of the 3-sphere adapted to the Hopf fibration.

$$g_{ij}^{\mathrm{Hopf}} = \frac{1}{4}\begin{pmatrix} 1 & & \\ & 1 & \cos\theta \\ & \cos\theta & 1 \end{pmatrix}$$

The first two coordinates $(\theta, \varphi) \in [0, \pi] \times [0, 2\pi]$ describe the S^2 base of the Hopf fibration, while the third coordinate $\psi \in [0, 4\pi)$ describes the S^1 fibers.

Each fiber is a maximal circle on the S^3 and two fibers with different base point are linked circles.

The coordinate ρ runs in the radial direction of AdS and the boundary is described by the $\rho \to \infty$ limit.

The coordinate transformation between the two systems is given, in the Euclidean case, by

$$\begin{cases} y = \dfrac{e^\tau}{\cosh\rho} \\ x^i = e^\tau \tanh\rho\; \Omega^i \end{cases}$$

where

$$\Omega^1 = \sin\frac{\theta}{2}\sin\frac{\varphi-\psi}{2} \qquad \Omega^2 = \sin\frac{\theta}{2}\cos\frac{\varphi-\psi}{2}$$
$$\Omega^3 = \cos\frac{\theta}{2}\sin\frac{\varphi+\psi}{2} \qquad \Omega^4 = \cos\frac{\theta}{2}\cos\frac{\varphi+\psi}{2}$$

describe the embedding of the S^3 in the $\mathbb{R}^4$ Euclidean space.

We will use another coordinates system to describe the full $\mathrm{AdS}_5 \times S^5$ space

$$\mathrm{d}s^2 = \frac{R^2}{Y^2}\left(\delta_{\mu\nu}\mathrm{d}x^\mu \mathrm{d}x^\nu + \mathrm{d}z^2\right) + R'^2 \mathrm{d}\Omega_6^2.$$

When the two factor spaces have the same radius, we can rewrite the metric as

$$\mathrm{d}s^2 = \frac{R^2}{Y^2}\left(\delta_{\mu\nu}\mathrm{d}x^\mu \mathrm{d}x^\nu + \delta_{ij}\mathrm{d}Y^i \mathrm{d}Y^j\right) \tag{1.2}$$

where $Y^i = z\Omega_6^i$ and $Y^2 = z^2$. Then we see that for equal radii, the space is conformally flat.

1.2. BRANE CONSTRUCTION

The origin of the AdS_5/CFT_4 correspondence can be explained in term of branes construction. We start from the 10-dimensional $\mathcal{N} = 1$ string theory, which has 16 supercharges. We can insert non-dynamical branes and consider the low energy theory on the branes.

Considering the perturbative excitations of the strings in this background, we have both close and open strings. Open strings whose both endpoints lie on the same brane (or on coincident branes) have arbitrarily short length, thus, from the low energy theory point of view, their ground states represent massless fields on the brane.

The excitations of the open strings induce a gauge theory on the worldbrane. Considering a $D3$-brane, we find an effective $U(1)$ gauge theory in four dimensions and since the brane breaks half of the supersymmetry it leaves an $\mathcal{N} = 4$ Poincaré supersymmetry in four dimensions.

If we take a stack of $D3$-branes the low energy degrees of freedom will be N distinct $U(1)$ gauge fields. Taking the N branes to coincide, we can built a non-abelian gauge theory. In this limit, in fact, the strings extending between two different branes become massless, hence the gauge symmetry is enhanced from $U(1)^N$ to $SU(N) \times U(1)$, where the $U(1)$ trivial factor parametrizes the position of the stack. The low energy theory therefore turns out to be $\mathcal{N} = 4$ SYM with $SU(N)$ gauge group living on the 4-dimensional worldvolume of the branes. The low energy effective action can then be decomposed as

$$S_{\text{eff}} = S_{\text{bulk}} + S_{\text{SYM}} + S_{\text{int}}$$

where S_{bulk} is the type IIB supergravity on the flat 10-dimensional space describing the close strings and S_{int} describes the interactions between the brane modes and the bulk gravity modes and it vanishes in the low energy limit $\alpha' \to 0$ since it is proportional to $\kappa = g_s \alpha'^2$. Hence, in the low energy limit, we have two decoupled theories: a 10-dimensional type IIB supergravity and a 4-dimensional $\mathcal{N} = 4$ SYM gauge theory.

From the string theory point of view, the presence of the $D3$-branes deforms the background geometry. In supergravity approximation, decomposing the coordinates as $x^M = (x^\mu, y^i)$ the metric becomes

$$\mathrm{d}s^2 = f(r)^{-1/2} \eta_{\mu\nu} \mathrm{d}x^\mu \mathrm{d}x^\nu + f(r)^{1/2} (\mathrm{d}r^2 + r^2 \Omega_5^2)$$

where $f(r) = 1 + \frac{R^4}{r^4}$ and $r^2 = y^i y^i$ is the radial direction. The dilaton field defines the string coupling constant $e^\phi = g_s$ and the radius of curvature is fixed

$$R^4 = 4\pi g_s N \alpha'^2.$$

The theory also contains a self-dual 5-form

$$F^+_{(5)\lambda\mu\nu\rho\sigma} = \epsilon_{\lambda\mu\nu\rho\sigma\eta} \partial^\eta f(r)$$

whose flux is quantized in the compact directions of the S^5

$$\int_{S^5} F^+_{(5)} = N,$$

while all the other RR-forms and the antisymmetric tensor $B_{\mu\nu}$ are set to zero.

In the asymptotic limit $r \to \infty$, we recover the 10-dimensional flat space supergravity theory.

In the near horizon limit $r \to 0$, the metric seems to be singular. However, by the coordinate change

$$r = \frac{R^2}{y}$$

in the $y \to \infty$ limit, the metric

$$\mathrm{d}s^2 = \frac{R^2}{y^2}(\eta_{\mu\nu}\mathrm{d}x^\mu \mathrm{d}x^\nu + \mathrm{d}z^2) + R^2 \mathrm{d}\Omega_5^2$$

is the metric of $\mathrm{AdS}_5 \times S^5$ space in the Poincaré patch 1.1.2.

The low energy action can then be decomposed as

$$S_{\text{eff}} = S_{\text{bulk}} + S_{\text{near horizon}} + S_{\text{int}}$$

where S_{bulk} describes the string theory in the flat limit $r \to \infty$ and S_{int} describes its interaction with the near horizon region. Again, in the low energy limit the two regions decouple since near horizon excitations cannot reach the asymptotic region due to gravitational potential, while the asymptotic excitations incoming from the bulk are insensitive to the horizon because their wavelength is much bigger than the typical gravitational size of the branes, due to the redshift factor.

The two different decompositions of the low energy effective action of the type IIB string theory in the presence of $D3$-branes both consist of two non-interacting systems, one of which is a common free supergravity theory in the bulk. It is therefore natural to conjecture the equivalence of the other two parts, that is the $\mathcal{N} = 4$ four dimensional SYM and the type IIB superstrings on the $\mathrm{AdS}_5 \times S^5$ background.

In order to make the correspondence quantitative, we need to match the parameters of the two theories. The string theory seems to have a parameter α' which does not appears in the gauge theory and sets the string tension and all other scales. However, this is only a parameter if we compare it to other scales of the theory, since only relative scales are meaningful. In fact only the ratio of the curvature radius over α' is a parameter, thus α' will disappear from any physical quantity we compute in this theory. The matching of the parameters is given by

$$g_s = g_{YM}^2$$

while the curvature radius of $\mathrm{AdS}_5 \times S^5$ space is fixed by

$$\frac{R^4}{\alpha'^2} = 4\pi g_s N. \tag{1.3}$$

It is possible to consider weaker limits for the equivalence. First of all, we can consider the large N limit. In $\mathcal{N} = 4$ SYM this is the famous 't Hooft limit, in which only planar Feynman diagrams contribute to the perturbative expansion. Because of (1.3), keeping the radius of curvature fixed, the large N limit corresponds to a weakly interacting string theory $g_s \to 0$. Non-planar diagrams contribute to $1/N$ corrections that correspond to higher genus worldsheets in the string theory. We will concentrate on the planar large N limit, where the theory is thought to be integrable.

The construction above is in no way a proof of the correspondence, since it relies on supergravity approximation. The supergravity description is only reliable when the radius of curvature of the background is big with respect to the string scale

$$\frac{R^4}{l_s^4} = g_s N = \lambda \gg 1.$$

The argument above is therefore solid only in the $N \to \infty$ and $\lambda \gg 1$ limit, which is the weakest form of the conjecture.

We notice that this is precisely the regime where perturbative computations fail, since in large N limit the relevant coupling constant for the field theory is λ. The gauge theory perturbative regime $\lambda \ll 1$ corresponds instead to the strongly coupled string theory. The correspondence is therefore a strong-weak duality, making it both extremely powerful in producing results otherwise inaccessible and extremely hard to proof, since the comparison of the results from the two theories is not straightforward.

1.3. SYMMETRIES MATCHING

The string theory on the $\mathrm{AdS}_5 \times S^5$ background[5] has a obvious $SO(2,4) \times SO(6)$ symmetry, that corresponds to the isometries of the target space. Actually, when considering supersymmetry, we need to deal with spinors, thus the relevant groups are the covering group $SU(2,2)$ and $SU(4)$ of $SO(2,4)$ and $SO(6)$ respectively. The string theory also contains 32 Majorana spinors supercharges, transforming in the fundamental of the bosonic group. Thus the full symmetry of the theory is given by a $PSU(2,2|4)$ supergroup. The string theory also exhibits a global $SL(2,\mathbb{Z})$ symmetry.

As already mentioned above, $\mathcal{N} = 4$ SYM theory is a conformal theory at quantum level. Hence it has an $SO(2,4)$ symmetry group. Moreover the theory contains six scalar fields and four spinor fields transforming in the **6** and **4** respectively of the $SU(4)$ R-symmetry group. Again, the bosonic and fermionic symmetries combine to a full $PSU(2,2,|4)$ supergroup. The

theory also shows an electric-magnetic duality of the complex coupling constant

$$\tau = \frac{\theta}{2\pi} + \frac{4\pi i}{g^2_{\mathrm{YM}}}$$

where θ is the instanton angle, whose group is $SL(2,\mathbb{Z})$, exactly matching the global symmetry of the string theory.

The two theories share the same symmetry, hence we can try to match the physical degrees of freedom, that is the actual representations of the symmetry supergroup.

1.4. AdS/CFT DICTIONARY

The most interesting quantities to compute in a conformal field theory are correlation functions.

The most studied among these are correlation functions of gauge invariant local operators

$$\mathcal{O}_I(x) = \mathrm{Tr}\,(\Phi_I \dots \Psi \dots F_{\mu\nu}) \tag{1.4}$$

where all fields are evaluated at the point x. In our case, the fields appearing in the operator are the fundamental fields of $\mathcal{N}=4$ supermultiplet (A_μ, ψ^a, Φ_I) and their derivative D_μ.

These operators are classified according to their conformal dimension Δ_I, that is their eigenvalue with respect to the scaling operator D. This means that under scaling transformations $x^\mu \to \lambda x^\mu$ they transform as

$$\mathcal{O}_I(x) \to \lambda^{\Delta_I}\mathcal{O}_I(\lambda x)$$

The commutation relations of the algebra (see appendix A) imply that $P_{\alpha\dot\alpha}$ raises the dimension of the operator, while $K^{\alpha\dot\alpha}$ lowers it. In any unitary field theory there is a lower bound to the dimension of local operators. Therefore, each representation of the conformal group must have a lowest dimension operator, which is annihilated by $K^{\alpha\dot\alpha}$. Such operators are called primary operators. All other operators can be built applying a certain number of generators $P_{\alpha\dot\alpha}$ to the primary operators and are called descendants.

Since the conformal group is much larger than the Poincaré group, the correlation functions of local operators are highly constrained by the symmetry of our theory.

Taking a orthogonal basis for the operators, the 2-point functions are completely fixed (up to a normalization constant)

$$\langle \mathcal{O}_I(x_I)\mathcal{O}_J(x_J)\rangle = \frac{\delta_{IJ}}{|x_I - x_J|^{2\Delta}}.$$

In general, for an interacting theory, the conformal dimension $\Delta_I(\lambda)$ is a function of the 't Hooft coupling constant, since for generic operators can receive quantum corrections.

For a special class of operators, which are annihilated by some combinations of the supercharges, the symmetry forbids radiative corrections. In fact, since the operator is annihilated by all S and some Q generators, we can use the commutation relations $\{Q, S\}$ to compute the eigenvalue Δ_I of D in term of Lorentz and R-symmetry representations. These protected operators are called chiral primary operators (CPO). The representations corresponding to chiral primary operators are smaller than the generic ones, containing less conformal fields.

Following this observation, the operators can be classified depending on the behavior of their scale dimension at large λ. Protected operators have dimensions of order one and thus they are said light, whereas non-protected operators whose dimensions scale as $\sqrt{\lambda}$ are said heavy.

The spatial dependence of 3-point functions is also completely fixed by symmetry

$$\begin{aligned} \langle \mathcal{O}_I(x_I)\mathcal{O}_J(x_J)\mathcal{O}_K(x_K)\rangle = \\ = \frac{c_{IJK}}{|x_I - x_J|^{\Delta_I+\Delta_J-\Delta_K}|x_J - x_K|^{\Delta_J+\Delta_K-\Delta_I}|x_I - x_K|^{\Delta_I+\Delta_K-\Delta_J}} \end{aligned} \tag{1.5}$$

However, the structure constant $c_{IJK}(\lambda)$ must be computed by other methods.

In order to compute the strong coupling expectation value of this correlation functions[6], we need to match the operators with the string states. This can be achieved by holographic principle, which states that the string theory is in contact with the field theory only through boundary terms.

Working in Poincaré patch, the metric diverges at the boundary $y = 0$. The scale factor can be removed by a Weyl rescaling of the metric, but this rescaling is not unique. In order to have a well defined limit, we need to consider a scale invariant theory on the boundary. This is exactly the case for $\mathcal{N} = 4$ SYM, so we can consider it to live on the boundary of AdS.

Consider a field living on $\mathrm{AdS}_5 \times S^5$. The field can always be expanded in spherical harmonics

$$\varphi(y, x^\mu, \Omega^I) = \sum_{\Delta=0}^{\infty} \varphi_\Delta(y, x^\mu) Y_\Delta(\Omega^I).$$

The field compactified on S^5 receives contribution to the mass, depending on the spin. For instance, scalar fields have a mass $m^2 = \Delta(\Delta - 4)$.

Assuming the fields to be asymptotically free, the two independent solutions to the wave equation have the asymptotic behavior

$$\varphi_\Delta(y, x^\mu) = \begin{cases} y^\Delta & \text{normalizable} \\ y^{4-\Delta} & \text{non-normalizable} \end{cases}$$

The normalizable solution corresponds to bulk excitations.

The non-normalizable solution instead corresponds to coupling of the supergravity or string theory fields to the external sources, that are the boundary fields. These are defined by

$$\varphi^0_\Delta(x^\mu) = \lim_{y\to 0}\ \varphi_\Delta(y, x^\mu) y^{4-\Delta}.$$

The prescription of the correspondence is that the generating function of the correlators of operators in the conformal theory is then equal to the classical string action

$$\left\langle e^{\int \mathcal{O}\varphi^0_\Delta(x)} \right\rangle = e^{-S(\varphi_{cl})}$$

evaluated on the configurations φ_{cl} that are the classical solutions to the equations of motion for the string action.

The knowledge of the 2 and 3-point functions of all the operators of the theory allows, at least in principle, to compute all the other correlation functions in a conformal field theory, using the operator product expansion (OPE)

$$\langle \mathcal{O}_I(x)\mathcal{O}_J(0)\rangle = \sum_K c_{IJ}{}^K \mathcal{O}_K(0) x^K.$$

Starting from this observation, we are prompted to compute 3-point functions of non protected operators. The main result of this work is the computation of the 2-point function of Wilson loops which is a preparatory step in this direction.

1.5. Integrability

In $\mathcal{N} = 4$ SYM, the problem of computing the spectrum of local operators of the theory at quantum level in the planar limit has been completely solved by integrability techniques [2], while the computation of 3-point functions is not yet fully understood.

The scaling dimensions of the operators are usually given as the solution of a set of integral equations, that follows from the thermodynamic Bethe ansatz (TBA). The equations have been solved numerically for a wide range of λ. In certain limits, the equations simplify to a set of algebraic equations (asymptotic Bethe equations) and can be solved analytically.

Integrability techniques have up to now been applied only to $\mathcal{N} = 4$ SYM. Any other 4-dimensional field theory however can be viewed as $\mathcal{N} = 4$ SYM with some particles and interactions added or removed. Several quantities, in fact, show a universal behavior for all the theories. This is the case for tree level scattering amplitudes and higher "trascendentality" part. Moreover, $\mathcal{N} = 4$ SYM acts as a representative model and selected results have been carried over to general gauge theories.

1.6. WILSON LOOPS AND MINIMAL SURFACES

Besides correlation functions of local operators, other interesting observables in a gauge theory are Wilson loops. These are defined as the holonomy of the gauge connection along close path

$$W_R(\mathcal{C}) = \frac{1}{d_R} \operatorname{Tr}_R \mathcal{P} \exp \oint_{\mathcal{C}} A_\mu \mathrm{d}x^\mu \tag{1.6}$$

where R is the representation of the gauge group on which the loop lives, and d_R its dimension.

In $\mathcal{N} = 4$ SYM, in order to preserve some of the supersymmetries, the loop must couple to a "twisted" connection that mixes the gauge connection and the scalar fields of the theory. The number of preserved charges depends on the minimal dimension of the space where the loop can be embedded. In the framework of AdS/CFT correspondence, the Wilson loop is a privileged observable, since it's conjectured to be dual to the fundamental string.

We will concentrate on a particular case of Wilson loops defined in [7] where the loop live on a 3-sphere. These loops live on a Hopf fibration of the 3-sphere, that is a way to locally describe the 3-sphere as a product $S_3 = S_2 \times S_1$. Any number of these loops, belonging to the same fibration, preserves 1/4 of the super-charges. Then the whole correlator is expected to be supersymmetric, hence protected against radiative correction, but has a non-trivial dependence on the 't Hooft coupling constant λ.

An infinitely massive quark in the fundamental representation moving along a path will be transformed by a phase factor 1.6. Thus the Wilson loop measures the effects of gauge dynamics on external sources: in particular for a parallel quark-antiquark pair, the Wilson loop is the exponent of the effective potential between the quarks and provides an order parameter for confinement[8].

In $\mathcal{N} = 4$ SYM there are no quarks in the fundamental representation, so we must consider a more general definition. To construct an infinitely massive particle in the fundamental representation, we consider again the derivation from the 10-dimensional string theory. Consider a stack of $N + 1$ D3-branes. Taking a single brane far apart from the stack, in the low energy limit, we can ignore all the fields on the distant brane except the open strings stretching between it and the other branes. From the point of view of low energy effective theory on the stack of the D3-branes, the open string is an infinitely massive W-boson in the fundamental representation of the $SU(N)$ gauge group.

From this construction, it appears natural to couple the loop operator not only to the 4-dimensional vector field, but also to the six scalar fields that comes from the dimensional reduction of the 10-dimensional vector. A

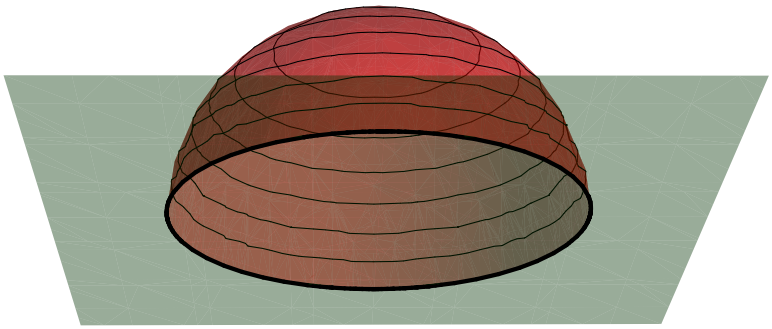

FIGURE 1.1: The Wilson loop (black thick line) at the boundary of AdS (green surface) and its dual fundamental string worldsheet (red surface). The string surface reaches the boundary of AdS, where it ends on the loop.

more general definition for the Wilson loop is then

$$W_R(\mathcal{C}) = \frac{1}{d_R} \operatorname{Tr}_R \mathcal{P} \exp \oint_{\mathcal{C}} \mathrm{d}t \left(i A_\mu \dot{x}^\mu + |\dot{x}| \theta^I \Phi_I \right) \tag{1.7}$$

The θ^I are the scalar couplings. In order to ensure supersymmetry locally at each point of the loop, they must parametrize a 5-sphere, $\theta^I \theta^I = 1$. The global supersymmetry imposes additional constraints depending on the loop shape.

We can perform a topological twisting of the gauge connection relating the couplings with the scalars to the one with the vector field. In this way we can define particular classes of loops.

In [9], Zarembo built a class of loops preserving pure supersymmetric charges. Because of this, they all have trivial expectation value, independent of the coupling constant. We will concentrate on a similar construction which however involves loops that preserve linear combinations of supersymmetric and superconformal charges. These loops have nontrivial expectation value due to the conformal anomaly. In particular, following [7], we consider loops lying on an $S^3 \subset \mathrm{AdS}_5$ and coupling to the scalars through the right invariant forms on an $S^3 \subset S^5$. We will discuss this in chapter 2.

We will focus on the computation of Wilson loops and their correlators in the strongly coupled regime. This can be done thanks to the AdS/CFT correspondence. According to the correspondence dictionary, the Wilson loop is dual to a fundamental open string whose boundary conditions are determined by the presence of the loop. In particular, the worldsheet ends, at the boundary of AdS, on the loop itself. The computation of the expectation

value would imply the solution of a complicated σ-model.

$$\mathcal{Z} = \int \mathcal{D}X^\mu \mathcal{D}h_{\alpha\beta} \mathcal{D}\vartheta^a \exp\left(-\frac{\sqrt{\lambda}}{4\pi}\int \mathrm{d}^2\sigma \sqrt{h} h^{\alpha\beta} G_{MN} \partial_\alpha X^M \partial_\beta X^N + \text{fermions}\right)$$

However, at leading order, the integral can be evaluated by saddle-point method. Then the problem of computing the expectation value of the Wilson loop reduces to the computation of the area of the surface ending on the loop at the boundary that minimizes the Polyakov action

$$S = \int \mathrm{d}^2\sigma \sqrt{h} h^{\alpha\beta} G_{MN} \partial_\alpha X^M \partial_\beta X^N.$$

The leading term of the expectation value at strong coupling $\lambda \gg 1$ is then

$$\langle W(\mathcal{C}) \rangle = \int_{\partial X = \mathcal{C}} \mathcal{D}X \exp\left(-\sqrt{\lambda}\mathcal{S}[X,Y]\right)\left(1 + \mathcal{O}\left(\frac{1}{\sqrt{\lambda}}\right)\right) \tag{1.8}$$

$$\sim \exp\left(-\sqrt{\lambda}\,\mathrm{Area}(\mathcal{C})\right) \tag{1.9}$$

where the presence of the loop $\mathcal{C}$ imposes the boundary conditions.

In particular, since the loop lives on a (stack of) $D3$-branes, the open string must obey four Dirichlet and six Neumann boundary conditions. If we describe the loop by (x^μ, y^I), by symmetry the x^μ impose Dirichlet boundary condition and y^I impose Neumann boundary conditions on the string worldsheet described by (X^μ, Y^I).

Taking the metric (1.2) and the worldsheet coordinates (σ^1, σ^2) such that the AdS boundary is located at $\sigma^1 = 0$, the boundary conditions are

$$X^\mu(0, \sigma^2) = x^\mu(\sigma^2) \tag{1.10}$$

$$j_2{}^a \partial_a Y^I(0, \sigma^2) = \dot{y}^I(\sigma^2) \tag{1.11}$$

where $j_a{}^b$, $(a, b = 1, 2)$ is the complex structure on the string worldsheet coming from the induced metric h_{ab}

$$j_a{}^b = \frac{1}{\sqrt{h}} h_{ac} \varepsilon^{cb}.$$

The string worldsheet needs to end on the boundary of AdS, in order to be dual to a Wilson loop. This imposes additional Dirichlet conditions

$$Y^I(0, \sigma^2) = 0$$

that are only compatible with the Neumann ones if the loop variables obey

$$\dot{x}^2 - \dot{y}^2 = 0. \tag{1.12}$$

In this case the Neumann boundary conditions can be written as Dirichlet boundary conditions on a S^5. Set $Y^I = Y\Theta^I$, then $\Theta^2 = 1$, that is $\Theta^I \in S^5$.

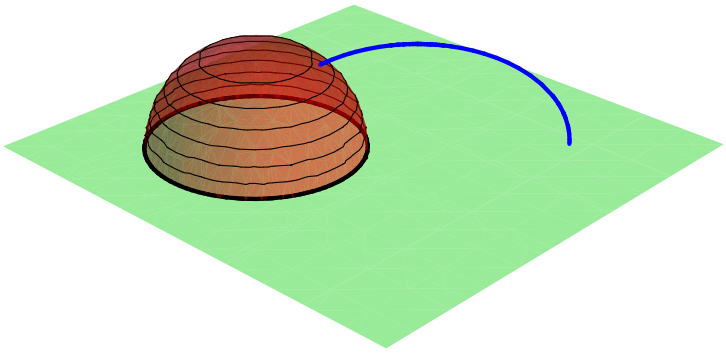

FIGURE 1.2: The correlation function of a Wilson loop with a light local operator is computed by the insertion of the corresponding vertex operator on the worldsheet (red surface) of the string dual to the loop. A bulk-to-boundary propagator (blue line) connects the insertion point with the local operator at the boundary of AdS.

Since at the boundary we have $\partial_a Y^i = (\partial_a Y)\Theta^I$ the Neumann boundary conditions becomes

$$\Theta^I(0,\sigma^2) = \frac{\dot{y}^I}{|\dot{y}|} = \theta^I(\sigma^2)$$

where $\dot{y}^I = |\dot{x}|\theta^I$

1.7. Mixed correlation functions and local operator insertion

Besides local operator and Wilson loops, mixed correlation functions can be studied [10][11]. These quantities are interesting because they provide informations on the loop and allow to decompose the loop itself on a basis of local operators

$$\frac{W_R(\mathcal{C})}{\langle W_R(\mathcal{C})\rangle} = 1 + \sum_K c^K r^{\Delta_K} \mathcal{O}_K(0) + \dots$$

when its characteristic size r is small with respect to the distance with a probe operator.

These quantities can be computed both at weak coupling, by standard perturbative expansion, and at strong coupling, by AdS/CFT correspondence. When the local operator is heavy, the string surface is modified in

order to attach to the operator on the boundary. Conversely, when the local operator is light, i.e. its dimension doesn't scale with the coupling constant, the string surface is not modified and the expectation value $\langle W_R(\mathcal{C})\mathcal{O}_I\rangle$ at strong coupling can be obtained by inserting the vertex operator associated to $\mathcal{O}_I$ on the worldsheet of the fundamental string dual to the Wilson loop and propagating it to the local operator at the boundary with a bulk-to-boundary propagator.

At the leading order, the correlation function with more light local operators factorizes in the product of the insertion of single operators with independent propagators, since the insertion of a single operator with a 3-point interaction on the propagator is subleading.

1.8. MAIN RESULTS FROM THE CORRESPONDENCE

The AdS/CFT correspondence, although it is still a conjecture and it has no rigorous proof, enlighted many striking features of the field theory and prompted to the discovery of unexpected relation between the observables of the theory itself.

One of the first impressive results was the computation of the quark-antiquark potential at strong coupling [12]. The potential is the logarithm of the expectation value of a degenerate rectangular $T \times L$ Wilson loop, in the limit where the temporal direction T is infinitely extended

$$\langle W(T,L)\rangle = e^{-TV(L)}.$$

Computing the Wilson loop expectation value with the prescription presented in 1.6, it was found that

$$V(L) = \frac{4\pi^2}{\Gamma(1/4)}\frac{\sqrt{\lambda}}{L}$$

where the $\sqrt{\lambda}$ behavior enlights a screening effect for the charge. We will return on this in 3.1.3

One of the most striking results is the discovery of a new symmetry of the $\mathcal{N} = 4$ SYM scattering amplitudes. This symmetry has a dynamical origin and is not manifest in the Lagrangian formulation. From the string theory point of view, it was noticed that the gluon scattering amplitudes can be computed at strong coupling by performing a T-duality transformation [13][14]. The problem is then mapped to the search of a minimal surface ending on a light-like polygon on the boundary of AdS. This is completely equivalent to the computation of the expectation value of a null polygonal Wilson loop. It was conjectured [15] and then proved [16] that the equivalence is also true at weak coupling. This was made possible by noting that the conformal symmetry of the T-dual Wilson loop is mapped to a hidden

(dual) conformal symmetry of the scattering amplitudes. The symmetry is exact at tree level, while it is broken at loop level. However the anomaly is under full control by Ward identities and it shows a universal behavior throughout a class of scattering amplitudes: the anomaly is the same for MHV (maximally helicity violating) and next-to-MHV amplitudes, so that their ratio is indeed conformally invariant.

Taking advantage of this new symmetry, it has been possible to express all the on-shell scattering amplitudes in a compact form by means of dual conformal invariant functions. Moreover, the cusp anomalous dimension, originally associated to the ultraviolet logarithmic divergence of a cusped Wilson loop, was understood to be a universal quantity that is also related to the infrared divergence of the scattering amplitudes and of correlation functions of local operators sitting on light-like separated edges [17][18][19].

Other important fields of application of the duality are in thermodynamics, hydrodynamics and condensed matter. AdS/CFT at finite temperature allowed to compute the entropy density and the shear viscosity of the $\mathcal{N} = 4$ gluon plasma [20][21]. The entropy can be computed by the Bekenstein-Hawking formula as the area of the black hole horizon

$$S_{\mathrm{BH}} = \frac{A}{4G} = \frac{\pi^2}{2} N^2 T^3.$$

The shear viscosity is obtained in the linear response approximation from the retarded correlator of two energy-momentum tensors, which correspond to the second functional derivative of the generating functional with respect to the source that couples to energy-momentum tensor itself. From AdS/CFT prescription, the generating functional of the gauge theory corresponds to the one of the string theory and the energy-momentum tensor is dual to the metric $g_{\mu\nu}$. Then schematically we have

$$\langle TT \rangle = \frac{\delta^2}{\delta h^2} S_{\mathrm{SuGra}}[g+h]\Big|_{h=0}$$

and the result for the viscosity is

$$\eta = \frac{\pi}{8} N^2 T^3$$

where T is the temperature.

More recently, charged AdS/CFT at finite temperature has been used to compute interesting observables in condensed matter physic. In particular, charged black holes gave new insight to the superconductors [22] and non-Fermi liquid [23] physics.

Chapter 2

Wilson Loops and Supersymmetry

2.1. BPS configurations

As explained in (1.7), the Wilson loop in $\mathcal{N}=4$ SYM can be coupled also to the scalars

$$W_R(\mathcal{C}) = \frac{1}{N_C}\operatorname{Tr}_R \mathcal{P}\exp\oint_{\mathcal{C}} \mathrm{d}t\left(iA_\mu \dot{x}^\mu(t) + |\dot{x}|\Theta^I(t)\Phi_I\right) \tag{2.1}$$

where $x^\mu(t)$ is the path of the loop and $\Theta^I(t)$ are arbitrary couplings of the loop with the scalars.

These extra couplings are needed in order to define a supersymmetric object. To this aim, we must in first place require that the norm of Θ^I is one. This will ensure that the supersymmetry is preserved locally.

When we consider the supersymmetry of the loop, then each point imposes different constraints. Only if all these constraints are satisfied the loop will be supersymmetric.

We can satisfy all the constraints at once, if the equation is the same at every point. For instance, this is the case for a straight line with constant scalar couplings, which is invariant under 1/2 of the supersymmetry charges. A generalization of this was constructed by Zarembo [9] by assigning to each vector in $\mathbb{R}^4$ a vector in the space of fields $\mathbb{R}^6$ by a 6×4 matrix as

$$|\dot{x}|\Theta^I = M^I{}_\mu \dot{x}^\mu.$$

This constructions ensures that a generic curve preserves 1/16 of the supersymmetry charges, while a curve contained in $\mathbb{R}^3$ preserves 1/8 of the supersymmetry and a curve contained in $\mathbb{R}^2$ preserves 1/4 of the supersymmetry.

This construction can be associated to a topological twist of $\mathcal{N}=4$ SYM, where we identify an $SO(4)$ subgroup of the $SO(6)_R$ R-symmetry group with

the Euclidean Lorentz group. Under this twist, four of the scalars become a space-time vector $\Phi_\mu = M^I{}_\mu \Phi_I$ and the Wilson loop is defined starting from the modified connection

$$A_\mu \to A_\mu + i\Phi_\mu.$$

All the loops defined in this way share an amazing property: their expectation values are all trivial. This result comes from both perturbative computations (weak coupling) and string theory dual (strong coupling).

2.2. ZAREMBO SUPERSYMMETRIC LOOPS

The supersymmetric variation of the Wilson loop is

$$\delta_\epsilon W(x,\theta) = \frac{1}{N} \operatorname{Tr} \mathcal{P} \oint_{\mathcal{C}} \mathrm{d}s\, \bar{\Psi}\big(i\Gamma_\mu \dot{x}^\mu + \Gamma_I \theta^I |\dot{x}|\big)\, \epsilon\, \exp \oint_{\mathcal{C}} \mathrm{d}s' \left(iA_\mu \dot{x}^\mu + \Phi_I \theta^I |\dot{x}|\right)$$

Some part of the supersymmetry will be preserved if

$$\big(i\Gamma_\mu \dot{x}^\mu + \Gamma_I \theta^I |\dot{x}|\big)\, \epsilon = 0. \tag{2.2}$$

Since the linear combination in bracket squares to zero, the equation has eight independent solutions for any s. In general, this solutions will depend on s, so an arbitrary Wilson loop is only locally supersymmetric. The requirement that ϵ is constant with respect to s is a constraint on $x^\mu(s)$ and $\theta^I(s)$. The number of linearly independent ϵ's satisfying eq. (2.2) is the number of conserved supercharges.

If θ^I are constants, (2.2) has no solutions, unless $\mathcal{C}$ is a straight line. Indeed, choosing a parametrization such that $|\dot{x}| = 1$ and differentiating in s, we get

$$i\Gamma_\mu \ddot{x}^\mu \epsilon = 0$$

which implies $\ddot{x} \equiv 0$.

For general θ^I, (2.2) is an infinite set of algebraic constraints for the sixteen unknown components of the 10-dimensional spinor ϵ. Despite the huge redundancy, nontrivial solutions for x^μ and θ^I exist.

By an ansatz, we can reduce (2.2) to a finite number of equations. The ansatz relates the position of the loop in S^5 to the tangent vector $\dot{x}^\mu$ of the space-time contour $\mathcal{C}$. The simplest way to map $S^3 \to S^5$ is to immerge $\mathbb{R}^4$ in $\mathbb{R}^6$ as an hyperplane

$$x^\mu \mapsto x^\mu M^I{}_\mu$$

where the 4×6 matrix $M^I{}_\mu$ can be regarded as a projection operator

$$M^I{}_\mu M^I{}_\nu = \delta_{\mu\nu}.$$

Because of $SO(4) \times SO(6)$ global symmetry, the particular form of the ${M^I}_\mu$ is irrelevant. Choosing

$$\theta^I = {M^I}_\mu \frac{\dot{x}^\mu}{|\dot{x}|}$$

the Wilson loop becomes

$$W_R(\mathcal{C}) = \frac{1}{N} \operatorname{Tr} \mathcal{P} \exp \oint_{\mathcal{C}} \mathrm{d}x^\mu \left(iA_\mu + {M^I}_\mu \Phi_I \right) \tag{2.3}$$

and the supersymmetry variation vanishes if

$$i\dot{x}^\mu \left(\Gamma_\mu - i{M^I}_\mu \Gamma_I \right) \epsilon = 0. \tag{2.4}$$

All the s-dependence factors out and we are left with four algebraic equations. To solve these equations we choose a basis in the spinor representation of $Spin(10)$. We can define four pairs of creation-annihilation operators

$$a^\mu = \frac{1}{2}(\Gamma_\mu - i{M^I}_\mu \Gamma_I)$$
$$a^{\mu\dagger} = \frac{1}{2}(\Gamma_\mu + i{M^I}_\mu \Gamma_I)$$

and a fifth pair can be constructed using two 6-vectors orthogonal to ${M^I}_\mu$

$$ {M^I}_\mu v_I^{(j)} = 0 \qquad {v_I^{(j)}}^2 = 1$$

$$a^4 = \frac{1}{2}(v_I^{(1)}\Gamma^I - iv_I^{(2)}\Gamma^I)a^{4\dagger} \qquad = \frac{1}{2}(v_I^{(1)}\Gamma^I + iv_I^{(2)}\Gamma^I).$$

The matrices a^M and $a^{M\dagger}$ satisfy anticommutation relations

$$\{a^M, a^{M\dagger}\} = \delta^{MN}$$

and their Fock space can be identified with the spinor representation of $Spin(10)$. The chirality projection separates states with even and odd number of creation operators acting on the Fock vacuum.

In this notation, (2.4) becomes

$$a^\mu |\varepsilon\rangle = 0$$

hence the levels associated with the a^μ, $\mu = 0, 1, 2, 3$ must be filled. There are two such states

$$|\epsilon_+\rangle = a^{0\dagger} \dots a^{3\dagger}|0\rangle$$
$$|\epsilon_-\rangle = a^{0\dagger} \dots a^{3\dagger} a^{4\dagger}|0\rangle$$

Dimensionality of the loop	Preserved supercharges	Supersymmetry
4D	1	1/16
3D	2	1/8
2D	4	1/4
1D	8	1/2

TABLE 2.1: Amount of supersymmetry for Wilson loops embedded in subspaces of various dimensions.

with opposite chirality. Hence there is only one Weyl spinor satisfying (2.4) and the Wilson loop operator commutes with one of the sixteen supercharges. Therefore a generic Wilson loop obtain by the ansatz (2.3) is 1/16 BPS.

If the contour $\mathcal{C}$ has special shape, the supersymmetry is enhanced. If a loop lies in a three dimensional slice, for instance $x^0 = c$, then $\dot{x}^0 \equiv 0$, so one of the constraints (2.4) is trivially satisfied and there are extra solutions

$$|\epsilon'_+\rangle = a^{1\dagger} \dots a^{3\dagger}|0\rangle$$
$$|\epsilon'_-\rangle = a^{1\dagger} \dots a^{3\dagger} a^{4\dagger}|0\rangle$$

Two out of four spinors are chiral, so the loop operator commutes with 2 supercharges and is a 1/8 BPS object.

If the loop lies in a two dimensional slice, the number of preserved supersymmetry again doubles and the loop operator is 1/4 BPS. Finally a one dimensional loop is the familiar Wilson line with constant θ^I, which is 1/2 BPS.

2.3. DGRT LOOPS

Beside the straight line, the circular Wilson loop is the other seminal example which is known to preserve half of supersymmetry. The expectation value of this loop is non-trivial since it depends on the 't Hooft coupling constant λ

$$\langle W_{\text{circle}} \rangle = e^{\sqrt{\lambda}}$$

The DGRT construction [7] is a generalization of this system, in the same way as the Zarembo construction is a generalization of the straight line.

In this case, we combine three of the scalar fields into a selfdual tensor

$$\Phi_{\mu\nu} = \sigma^i_{\mu\nu} M^I{}_i \Phi_I \tag{2.5}$$

and the Wilson loop is defined starting from the twisted connection

$$A_\mu \to A_\mu + i\Phi_{\mu\nu} x^\nu.$$

The tensors $\sigma^i_{\mu\nu}$, which are the key ingredients of this construction, can be thought in two different way.

They are the decomposition of the Lorentz generators in the anti-chiral spinor representation $\gamma_{\mu\nu}$ into Pauli matrices τ_i

$$\frac{1-\gamma_5}{2}\gamma_{\mu\nu} = i\sigma^i_{\mu\nu}\tau_i.$$

From another point of view, the $\sigma^i_{\mu\nu}$ tensors are the components of the right invariant 1-forms on the 3-sphere

$$\sigma^{(R)}_i = 2\sigma^i_{\mu\nu}x^\mu \mathrm{d}x^\nu$$

where

$$\begin{aligned}
\sigma^{(R)}_1 &= 2(x^2\mathrm{d}x^3 - x^3\mathrm{d}x^2 + x^4\mathrm{d}x^1 - x^1\mathrm{d}x^4)\\
\sigma^{(R)}_2 &= 2(x^3\mathrm{d}x^1 - x^1\mathrm{d}x^3 + x^4\mathrm{d}x^2 - x^2\mathrm{d}x^4)\\
\sigma^{(R)}_3 &= 2(x^1\mathrm{d}x^2 - x^2\mathrm{d}x^1 + x^4\mathrm{d}x^3 - x^3\mathrm{d}x^4)
\end{aligned} \tag{2.6}$$

This construction introduces a length scale: the tensor (2.5) has mass dimension one instead of two. Then the loop is supersymmetric only if we take the loop to lie on a 3-sphere. This sphere may be embedded in $\mathbb{R}^4$ or be a fixed-time slice of $S^3 \times \mathbb{R}$.

We will consider Wilson loops of the form

$$W = \frac{1}{N}\,\mathrm{Tr}\,\mathcal{P}\exp\oint \mathrm{d}x^\mu \left(iA_\mu - \sigma^i_{\mu\nu}x^\nu M^I{}_i\Phi_I\right) \tag{2.7}$$

The supersymmetry variation of the loop is then

$$\delta W \simeq \left(i\dot{x}^\mu\gamma_\mu - \sigma^i_{\mu\nu}\dot{x}^\mu x^\nu M^I{}_i\rho_I\gamma_5\right)\epsilon(x)$$

where γ_μ and ρ_I are the gamma matrices of the Poincaré group $SO(4)$ and of the R-symmetry group $SO(6)$ and $\epsilon(x)$ is a conformal-Killing spinor

$$\epsilon(x) = \epsilon_0 + x^\mu\gamma_\mu\epsilon_1$$

with ϵ_0 and ϵ_1 arbitrary constant 16-components Majorana-Weyl spinors.

Without loss of generality, taking advantage of the $SO(6)$ rotational symmetry of the scalars, we can fix $M^I{}_i = \delta^I_i$. This is a choice of the three scalars that will couple to the loop and breaks $SO(6) \simeq SU(4)$ to $SU(2)_A \times SU(2)_B$. Using the fact that $x_\mu x^\mu = 1$, we can rewrite

$$\delta W \simeq i\dot{x}^\mu x^\nu\left(\gamma_{\mu\nu}\epsilon_1 + i\sigma^I_{\mu\nu}\rho_I\gamma_5\epsilon_0\right) - i\dot{x}^\mu x^\nu x^\lambda\left(\gamma_{\mu\nu}\epsilon_0 + i\sigma^I_{\mu\nu}\rho_I\gamma_5\epsilon_1\right)$$

Requiring the supersymmetry variation to vanish for a generic path on S^3 leads to the constraints

$$\gamma_{\mu\nu}\epsilon_1 + i\sigma^I_{\mu\nu}\rho_I\gamma_5\epsilon_0 = 0 \tag{2.8}$$

$$\gamma_{\mu\nu}\epsilon_0 + i\sigma^I_{\mu\nu}\rho_I\gamma_5\epsilon_1 = 0 \tag{2.9}$$

Decomposing the ϵ_0 and ϵ_1 into their chiral and antichiral components and imposing

$$\tau_I \epsilon_1^- = \rho_I \epsilon_0^-, \qquad \epsilon_1^+ = \epsilon_0^+ = 0 \tag{2.10}$$

we get three constraints consistent with each other

$$i\tau_1 \epsilon_1^- = -\rho_{23}\epsilon_1^- \qquad i\tau_2 \epsilon_1^- = -\rho_{31}\epsilon_1^- \qquad i\tau_3 \epsilon_1^- = -\rho_{12}\epsilon_1^-. \tag{2.11}$$

Among these constraints, only two are independent, since the commutator of any two gives the remaining equation. The spinor ϵ_1 has then two independent components, while ϵ_0 is completely determined by ϵ_1. Then a Wilson loop along a generic curve on S^3 preserves 1/16 of the original supersymmetries.

In order to explicitly compute the combinations of $\bar{Q}$ and $\bar{S}$ which leave the loop invariant, we begin noticing that the operators in (2.10) are the generators of $SU(2)_R$, the antichiral part of the Lorentz group, and of $SU(2)_A$. The equations then state that ϵ_1^- is a singlet in the diagonal sum of $SU(2)_R$ and $SU(2)_A$, while its a doublet under $SU(2)_B$. This means that we can choose a basis in which ρ_I acts as Pauli matrices on the $SU(2)_A$ indices, so that the equation becomes

$$\left(\tau_k^R + \tau_k^A\right) \epsilon_1^- = 0.$$

Splitting the $SU(4)$ index A

$$(\epsilon_1)_A^{\dot{\alpha}} = (\epsilon_1)_a^{\dot{a}\dot{\alpha}}$$

where $\dot{a}$ and a are $SU(2)_A$ and $SU(2)_B$ indices respectively, the solution to (2.3) is

$$\epsilon_{1a} = \varepsilon_{\dot{a}\dot{\alpha}} (\epsilon_1)_a^{\dot{a}\dot{\alpha}}$$

Then we can determine ϵ_0

$$\epsilon_0^- = \tau_3^R \rho_3 \epsilon_1^- = \tau_3^R \tau_3^A \epsilon_1^- = -\epsilon_1^- \tag{2.12}$$

Finally, the Wilson loop preserves two supercharges

$$\bar{\mathcal{Q}}^a = \varepsilon^{\dot{a}\dot{\alpha}} \left(\bar{Q}_{\dot{a}\dot{\alpha}}^a - \bar{S}_{\dot{a}\dot{\alpha}}^a\right)$$

The Wilson loops obviously also preserves the $SU(2)_B$ bosonic symmetry and by combining these two symmetry we generate an $OSp(1|2)$ subalgebra of the superconformal group.

2.3.1. Hopf fibers

The Hopf fibration is an S^1 bundle over S^2, that is we can locally decompose $S^3 = S^2 \times S^1$.

We can describe the fibration by means of tailored coordinates. Consider the S^3 embedded in the $\mathbb{R}^4$ flat space. We can parametrize it by the angular variables $(\theta, \varphi, \psi) \in [0, \pi] \times [0, 2\pi) \times [0, 4\pi)$

$$x^1 = \sin\frac{\theta}{2}\sin\frac{\varphi-\psi}{2} \tag{2.13}$$

$$x^2 = \sin\frac{\theta}{2}\cos\frac{\varphi-\psi}{2} \tag{2.14}$$

$$x^3 = \cos\frac{\theta}{2}\sin\frac{\varphi+\psi}{2} \tag{2.15}$$

$$x^4 = \cos\frac{\theta}{2}\cos\frac{\varphi+\psi}{2} \tag{2.16}$$

The Hopf map $\pi : S^3 \to S^2$

$$\pi : \begin{pmatrix} x^1 \\ x^2 \\ x^3 \\ x^4 \end{pmatrix} \mapsto \begin{pmatrix} 2(x^2x^4 - x^1x^3) \\ 2(x^2x^3 + x^1x^4) \\ (x^3)^2 + (x^4)^2 - (x^1)^2 - (x^2)^2 \end{pmatrix} = \begin{pmatrix} \cos\varphi\sin\theta \\ \sin\varphi\sin\theta \\ \cos\theta \end{pmatrix}$$

projects the S^3 on the S^2 base of the fibration. Hence the ψ coordinate parametrizes the S^1 fibers, while (θ, φ) parametrize the base S^2.

Each fiber is a maximal circle on S^3 and all the fibers in a fixed fibration are non-intersecting.

Describing the 3-sphere as an Hopf fibration is particularly interesting. A loop along a fiber will sit at constant (θ, φ), while ψ is the arc parameter of the curve. The interesting fact is that all fibers in the same fibration couple to the same scalar Φ^3 only. In fact the right invariant one forms in this case are

$$\sigma_1^{(R)} = -\sin\psi\,\mathrm{d}\theta + \cos\psi\,\sin\theta\,\mathrm{d}\varphi \tag{2.17}$$

$$\sigma_2^{(R)} = \cos\psi\,\mathrm{d}\theta + \sin\psi\,\sin\theta\,\mathrm{d}\varphi \tag{2.18}$$

$$\sigma_3^{(R)} = \mathrm{d}\psi + \cos\theta\,\mathrm{d}\varphi. \tag{2.19}$$

If θ and φ are constant and $\psi = 2t$, with $t \in [0, 2\pi)$, then

$$\sigma_1^{(R)} = \sigma_2^{(R)} = 0, \qquad \sigma_3^{(R)} = 2\mathrm{d}t.$$

A single fiber is a great circle on S^3, so the loop will preserve half of the supersymmetry. In fact, the vanishing of supersymmetry variation of the loop leads to a single constraint

$$\rho^3\gamma_5\varepsilon_0 = i\gamma_{12}\varepsilon_1$$

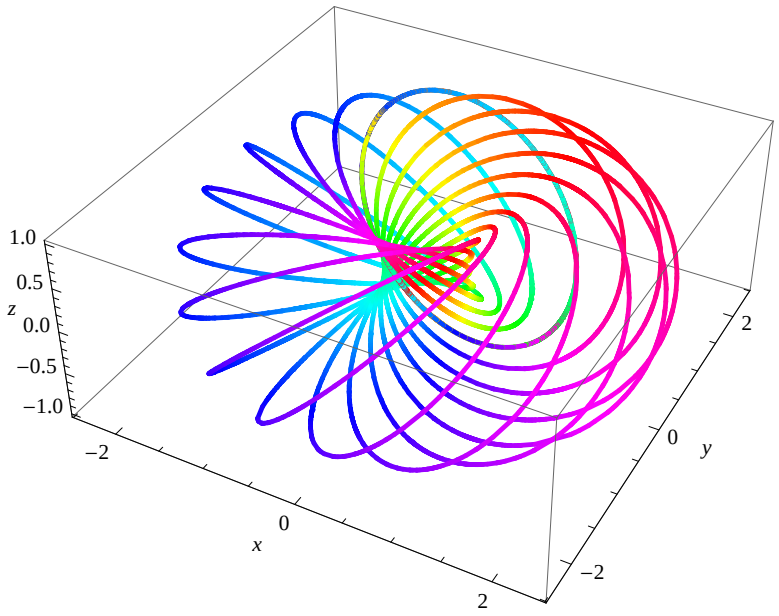

FIGURE 2.1: A stereographic projection of the Hopf fibration. All fibers are at the same θ and different φ on the base S^2. The colors correspond to the values of ψ along the fibers.

and therefore the loop itself preserves 8 chiral and 8 anti-chiral combinations of Q and S.

$$\mathcal{Q}^A = i\gamma_{12}Q^A + \left(\rho^3 S\right)^A \qquad \bar{\mathcal{Q}}_A = i\gamma_{12}\bar{Q}_A - \left(\rho^3 \bar{S}\right)_A .$$

The loop also preserve a bosonic symmetry $SL(2,\mathbb{R}) \times SU(2) \times SO(5)$. The $SO(5) \subset SO(6)$ invariance follows from the coupling to a single scalar field. The $SL(2,\mathbb{R}) \times SU(2) \subset SO(5,1)$ correspond to the group that leaves the loop invariant and is generated by

$$I_1 = \frac{1}{2}(P_1 + K_1) \qquad I_2 = \frac{1}{2}(P_2 + K_2) \qquad I_3 = J_{12} \tag{2.20}$$

$$L_1 = \frac{1}{2}(P_3 - K_3) \qquad L_2 = \frac{1}{2}(P_4 - K_4) \qquad L_3 = J_{34} \tag{2.21}$$

Considering two fibers, the second one will break some of the symmetry of the single loop. The generators of the residual symmetry preserved by the first loop act non-trivially one the second fiber. In particular, the $SL(2,\mathbb{R})$ generators allow us to map any point on the base, excluding $\theta = \pi$ where the first loop lies, to any other. Hence we can take the second loop at $\theta = 0$ and we are left with two constraints

$$\rho^3\gamma_5\varepsilon_0 = i\gamma_{12}\varepsilon_1 \qquad\qquad \rho^3\gamma_5\varepsilon_0 = -i\gamma_{34}\varepsilon_1. \tag{2.22}$$

In particular

$$\gamma_{12}\varepsilon_1 = -\gamma_{34}\varepsilon_1,$$

that is, ε_1 is anti-chiral and the loops preserve 1/4 of the supersymmetry.

The preserved supercharges are the ones with negative chirality among those preserving the single loop

$$\bar{\mathcal{Q}}_A = i\gamma_{12}\bar{Q}_A - \left(\rho^3\bar{S}\right)_A .$$

The remaining bosonic symmetry are the $U(1)$ rotations of the angle ψ as well as the $SO(5)$ rotations of the uncoupled fields.

2.4. Matrix model

For the circular Wilson loop, it is possible to show that the expectation value is computed exactly to all orders in perturbation theory by a matrix model[24][25].

This can be explained in the following way. The expectation value of the circle and of the straight line are different, although the two are related by a conformal transformation, because large conformal transformations (such as the invertion $x^\mu \mapsto -x^\mu/x^2$ are not symmetries of $\mathbb{R}^4$, since they map the point at the infinity to a point at finite distance. We might then guess that the difference in the expectation values is the contribution of the fields at a single point.

The expectation value of the circle, in fact, is equal to the Wilson loop of a large N Hermitian matrix model

$$\left\langle \frac{1}{N}\operatorname{Tr}\exp M \right\rangle = \frac{1}{Z}\int \mathcal{D}M \frac{1}{N}\operatorname{Tr}\exp M \ \exp\left(-\frac{2}{g^2}\operatorname{Tr}M^2\right) \tag{2.23}$$

and we can associate the field M to the fluctuations of the fields at the point at infinity.

The physical picture is the following: under a conformal transformation the gluon propagator is modified by a total derivative. This is a gauge transformation and naively it should not affect the expectation value of the Wilson loop, since it is gauge invariant. However, the gauge transformation is singular at the point that is mapped to infinity. The invariance of the loop is broken precisely at this point and the contributions of the singularities can be summed up in a matrix model.

In the case in exam, for $\mathcal{N} = 4$ SYM, the matrix model turns out to be Gaussian, hence we can compute the expectation value exactly to all orders in perturbation theory, for any coupling λ and any color number N.

This construction can be made rigorous by localization technique[26][27] and it is also valid for $\mathcal{N} = 2$ theories. To show that the path integral localizes, we add to the action particular term depending on a parameter t.

Let Q be a fermionic symmetry of the theory and $Q^2 = R$ a bosonic symmetry. Then the action S is invariant under Q, $QS = 0$. Consider a functional V invariant under R so that $RV = Q^2V = 0$. The deformation of the action by a Q-exact term QV can be written as a total derivative and a doesn't change the integral up to boundary terms

$$\frac{\mathrm{d}}{\mathrm{d}t}\int e^{S+tQV} = \int \{Q, V\} e^{S+tQV} = \int \{Q, Ve^{S+tQV}\} = 0.$$

In the limit $t \to \infty$, the integral is dominated by QV. For sufficiently nice V, the integral is computed by evaluating S at the critical points of QV and the corresponding 1-loop determinant. In this picture, the path integral localizes on the constant modes of the scalar field coupling to the Wilson loop, with all other fields vanishing.

Since the Wilson loops are Q-closed, the deformation of the action does not change their expectation value. Hence, when t goes to infinity, the theory localizes to some set $\mathcal{M}$ of critical points of QV over which we integrate at the end. The measure over $\mathcal{M}$ comes from the restriction of the action S to $\mathcal{M}$ and the determinant of the kinetic term of QV which counts the fluctuations in the normal direction to $\mathcal{M}$.

From localization, it has been possible to compute the expectation value of the circle to all orders. We start from the straight line

$$x^\mu(t) = \frac{1}{2}\left(1, \tan\left(\frac{t}{2}\right)\right),$$

which has trivial expectation value, meaning that the sum of all diagram vanishes. Mapping the line to the circle

$$x^\mu = (1 + \cos t, \sin t),$$

the point at the infinity is mapped to the origin. Then the only contributions come from the part of the diagram where both ends of a single propagator approach the origin and will give a constant factor.

This is possible because the sum of the gluon and the scalar propagators between two points on the circle is constant

$$\frac{\lambda}{16\pi^2}\int_0^{2\pi} \mathrm{d}t_1 \mathrm{d}t_2 \frac{-\dot{x}(t_1)\dot{x}(t_2) + |\dot{x}(t_1)||\dot{x}(t_2)|}{(x(t_1) - x(t_2))^2} = \frac{\lambda}{8}.$$

and, in Feynman gauge, only ladder diagrams contribute, while all the interacting diagrams combine to vanish. Then the sum of all diagrams reduce to the solution of the matrix model (2.23) and the final result is

$$\langle W_{\text{circle}} \rangle = \sum_{N=0}^{\infty} \frac{1}{N} L_{N-1}^1\left(-\frac{\lambda}{4N}\right) \exp\left(\frac{\lambda}{8N}\right) \tag{2.24}$$

where L_n^m are the Laguerre polynomial

$$L_n^m(x) = \frac{1}{n!} e^x x^{-m} \left(\frac{\mathrm{d}}{\mathrm{d}x}\right)^n \left(e^{-x} x^{n+m}\right).$$

At the leading order we find

$$\langle W_{\text{circle}} \rangle = \frac{2}{\sqrt{\lambda}} I_1(\sqrt{\lambda})$$

where $I_1(x) = \sum_{k=0}^{\infty} \frac{x^{n+2k}}{k!(n+k)!}$ is the modified Bessel function of the first kind. The result (2.24) is in agreement with the perturbative result at weak coupling

$$\langle W_{\text{circle}} \rangle = 1 + \frac{\lambda}{8} + \mathcal{O}(\lambda^2)$$

and has the correct exponential behavior at strong coupling to match the result from the gravity dual

$$\langle W_{\text{circle}} \rangle = e^{\sqrt{\lambda}}.$$

2.5. Calibrated surfaces

At strong coupling, the underlying geometry of the string solution is surprisingly simple. It turns out that the supersymmetry of the solutions is related to the existence of an almost complex structure on the subspace of $\mathrm{AdS}_5 \times S^5$ in which the string solution dual to the loop lives[28][29][7].

Supersymmetric string surfaces satisfy the pseudo-holomorphic equation associated to this almost complex structure.

Let Σ be a 2-dimensional surface with complex structure $j^\alpha{}_\beta$ embedded in a space $\mathcal{X}$ with almost complex structure $\mathcal{J}^M{}_N$. The surface is said pseudo-holomorphic if it satisfies

$$V_\alpha^M = \partial_\alpha X^M \mp \mathcal{J}^M{}_N j_\alpha{}^\beta \partial_\beta X^N = 0 \tag{2.25}$$

where the choice of the sign corresponds to the choice of holomorphic or anti-holomorphic embeddings.

Introducing the positive definite quantity

$$\mathcal{P} = \frac{1}{4} \int_\Sigma \sqrt{h} h^{\alpha\beta} G_{MN} V_\alpha^M V_\beta^N \geqslant 0$$

we have

$$\mathcal{P} = \mathrm{Area}(\Sigma) - \int_\Sigma \mathcal{J}$$

where $\mathcal{J}$ is the pull-back of the fundamental 2-form

$$\mathcal{J} = \frac{1}{2} \mathcal{J}_{MN} \mathrm{d}X^M \wedge \mathrm{d}X^N.$$

For a pseudo-holomorphic surface $\mathcal{P} = 0$, hence

$$\text{Area}(\Sigma) = \int_\Sigma \mathcal{J}$$

If $\mathcal{J}$ is closed, its integral is the same for all surfaces in the same homology class and the bound $\mathcal{P} \geqslant 0$ applies to all of them. Therefore, a string surface calibrated by a closed two-form is necessarily a minimal surface in its homology class.

In order to study supersymmetry, we interpret the two-form $\mathcal{J}$ as a bulk extention of the scalar couplings $\sigma^i_{\mu\nu}$. To this aim, we rewrite the supersymmetry constraint in terms of curved-space gamma matrices $\Gamma_M = (\Gamma_\mu, \Gamma_i) = (z^{-1}\gamma_\mu, z\rho_i)$ as

$$\begin{aligned} z\Gamma_{M\mu}\epsilon_0^- &= -i\mathcal{J}^N{}_{M;\mu}\Gamma_N\epsilon_0^- \\ z\Gamma_{Mi}\epsilon_0^- &= i\mathcal{J}^N{}_{M;i}\Gamma_N\epsilon_0^- \end{aligned} \tag{2.26}$$

with

$$\mathcal{J}^\mu{}_{\nu;i} = z^2\sigma^i_{\mu\nu}, \quad \mathcal{J}^\nu{}_{i;\mu} = -z^4\mathcal{J}^i{}_{\nu;\mu} = z^2\sigma^i_{\nu\mu}, \quad \mathcal{J}^i{}_{j;k} = -z^2\varepsilon_{ijk} \tag{2.27}$$

and all other components vanishing.

We can then introduce the matrix

$$\mathcal{J}^M{}_N = \mathcal{J}^M{}_{N;P}X^P$$

so that

$$\mathcal{J} = \begin{pmatrix} z^2\sigma^i_{\mu\nu}y^i & z^2\sigma^j_{\mu\nu}x^\nu \\ -z^{-2}\sigma^i_{\nu\mu}x^\mu & -z^2\varepsilon_{ijk}y^k \end{pmatrix}$$

$\mathcal{J}$ defines an almost complex structure on $\text{AdS}_4 \times S^2$ which reflects the topological twisting associated to the loop. The twisting reduces the product of the group $SU(2)_R$ and $SU(2)_A$ to their diagonal subgroup $SU(2)_{R'}$ which is then regarded as part of the Lorentz group. This is manifest from the condition

$$\left(\mathcal{J}^{\mu\nu}{}_{;i}\Gamma_{\mu\nu} - \mathcal{J}^{jk}{}_{;i}\Gamma_{jk}\right)\epsilon_0^- = 0$$

which expresses the invariance of ϵ_0 under the twisted $SU(2)_{R'}$ action

$$\left(\sigma^i_{\mu\nu}\gamma_{\mu\nu} + \varepsilon_{ijk}\rho_{jk}\right)\epsilon_0 = 0.$$

Introducing the vector $X^M = (x_1, x_2, x_3, x_4, y_1, y_2, y_3)$ we can write the pseudo-holomorphic equations associated to $\mathcal{J}$ as

$$\mathcal{J}^M{}_N\partial_\alpha X^N - \sqrt{h}\varepsilon_{\alpha\beta}\partial^\beta X^M = 0. \tag{2.28}$$

In the $z \to 0$ limit, as we approach the AdS_5 boundary, the lower left submatrix $\mathcal{J}^i{}_\nu$ dominates. Its entries are the components of the forms $\sigma_i^{(R)}$

which defines the coupling of the scalars Φ_I to the loop operator. Therefore $\mathcal{J}$ can be viewed as a bulk extension of those couplings.

We can introduce the fundamental 2-form

$$\mathcal{J} = \frac{1}{2}\mathcal{J}_{MN}\mathrm{d}X^M \wedge \mathrm{d}X^N = \frac{1}{4}y^i\left(\mathrm{d}\sigma^i - z^4\mathrm{d}\eta^i\right) - \frac{1}{2}\sigma^i \wedge \mathrm{d}y^i$$

where $\eta^i$are the pull-backs of the $SU(2)_A$ currents

$$\eta^1 = 2(y_2\mathrm{d}y_3 - y_3\mathrm{d}y_2) \tag{2.29}$$

$$\eta^2 = 2(y_3\mathrm{d}y_1 - y_1\mathrm{d}y_3) \tag{2.30}$$

$$\eta^3 = 2(y_1\mathrm{d}y_2 - y_2\mathrm{d}y_1) \tag{2.31}$$

This is not a standard calibration, since it's not closed

$$\mathrm{d}\mathcal{J} = -\frac{1}{4}\mathrm{d}y^i \wedge \mathrm{d}\sigma^i + z^4\mathrm{d}y_1 \wedge \mathrm{d}y_2 \wedge \mathrm{d}y_3.$$

Then we have to make sure that solutions of the pseudo-holomorphic equations are automatically solutions of the σ-model.

To this aim, consider the equations of motions for the σ-model in $\mathrm{AdS}_5 \times S^2$ (the equations of motion for the other S^5 coordinates are satisfied by setting them to constants)

$$\nabla_\alpha(G_MN\partial^\alpha X^N) = \partial_\alpha(G_{MN}\partial^\alpha X^N) - \frac{1}{2}\partial_M G_{PN}\partial_\alpha X^P\partial^\alpha X^n = 0$$

Assuming that the string lives in a $AdS_4 \times S^2$ subspace, a solution of the $\mathcal{J}$ equations satisfies also the equations of motion. Using $\mathcal{J}$-equation we have

$$\epsilon^{\alpha\beta}\partial_\alpha X^P\partial_\beta X^N\left(\partial_P\mathcal{J}_{MN} - \frac{1}{2}\partial_M G_{QP}\mathcal{J}^Q{}_N\right) = 0$$

When $M = \mu$ the second term vanishes and the condition is satisfied. When $M = i$ it becomes

$$\frac{1}{2}(\mathrm{d}\sigma^i - z^4\mathrm{d}\eta^i)(\delta^{ik} - z^2y^iy^k)$$

which vanishes by orthogonality condition $x^\mu\mathrm{d}x^\mu - z^4y^i\mathrm{d}y^i = 0$.

String worldsheet satisfying the $\mathcal{J}$-equations are supersymmetric and they are invariant under the same supercharges which annihilate the dual operator on the field theory.

To see this, consider a Killing spinor $\varepsilon_{\mathrm{AdS}}$ on $\mathrm{AdS}_5 \times S^5$

$$\epsilon_{\mathrm{AdS}} = \frac{1}{\sqrt{z}}\left(\epsilon_0 + z(x^\mu\Gamma_\mu - y^i\Gamma_i)\epsilon_1\right)$$

where ϵ_0 and ϵ_1 are constant 16-component Majorana-Weyl spinors. At the boundary, they are the analogue of the spinors representing Poincaré and

conformal supersymmetry in four dimensions, as we see in the boundary limit

$$\epsilon_{\text{AdS}} \underset{z\to 0}{\sim} \frac{1}{\sqrt{z}}(\epsilon_0 + x^\mu \gamma_\mu \epsilon_1)$$

We can write the κ-symmetry condition as

$$\left(\sqrt{g}\varepsilon^{\alpha\beta}\partial_\alpha X^M \partial_\beta X^N \Gamma_{MN} - iG_{MN}\partial_\alpha X^M \partial^\alpha X^N\right)\epsilon_{\text{AdS}} = 0$$

By equation (2.28), we can rewrite the term in brackets as

$$\partial^\alpha X^P \Gamma_P \partial_\alpha X^M \left(\mathcal{J}^N{}_M \Gamma_N - i\Gamma_M\right)$$

hence it will be enough to prove that

$$\partial_\alpha X^M \left(\mathcal{J}^N{}_M \Gamma_N - i\Gamma_M\right)\epsilon_{\text{AdS}} = 0 \tag{2.32}$$

This equation should be satisfied by the same parameters as in the gauge theory. Then taking $\epsilon_1^- = -\epsilon_0^-$ as in (2.12), we can rewrite

$$\begin{aligned} i\mathrm{d}X^M \left(-iX^P \mathcal{J}^N{}_{M;P}\Gamma_N \epsilon_0 + z(x^\mu \Gamma_{M\mu} - y^i \Gamma_{Mi})\epsilon_0\right) + \\ - i\mathrm{d}X^M \left(\Gamma_M \epsilon_0 - izX^P \mathcal{J}^N{}_{M;P}\Gamma_N (x^\mu \Gamma_\mu - y^i \Gamma_i)\epsilon_0\right) = 0 \end{aligned}$$

The first line vanishes immediately because of (2.26), while the second line vanish once we remember $x^2 + z^2 = 1$ and $x^\mu \mathrm{d}x^\mu - z^4 y^i \mathrm{d}y^i = 0$.

Hence, string worldsheets satisfying the equation (2.28) are supersymmetric and invariant under the same charges which annihilate the dual Wilson loop operator in the gauge theory.

From equation (2.32) we can get other interesting relation. Multiplying it by $\partial_{\bar{z}} X^P \Gamma_P$ we get

$$\partial_{\bar{z}} X^M \partial_{\bar{z}} X^M \epsilon_{\text{AdS}} = 0$$

which holds because of Virasoro constraints.

Multiplying by $\partial_z X^P \Gamma_P$ allows us to recast the κ-symmetry condition in the $(z, \bar{z})$ basis

$$-i\partial_z X^M \partial_{\bar{z}} X^N \left(\Gamma_{MN} + G_{MN}\right)\epsilon_{\text{AdS}} = 0$$

Finally, by pseudo-holomorphic equation we can rewrite (2.32) as

$$\partial_{\bar{z}} X^M \Gamma_M \epsilon_{\text{AdS}} = \Gamma_{\bar{z}} \epsilon_{\text{AdS}} = 0$$

where $\Gamma_{\bar{z}}$ is the pull-back of the gamma matrices on the string worldsheet.

Chapter 3

Strong coupling results

3.1. Basic examples

We will now present some early results about strong coupling computations of Wilson loops expectation values. This results, already present in the literature, allow to enlight some properties of the loops and to point out difference with our results.

3.1.1. Straight line

We can parametrize the infinite straight line as

$$x^\mu(\sigma_2) = (\sigma_2, 0, 0, 0)$$

By symmetry considerations, the minimal surface obeying to this boundary condition is an infinite plane orthogonal to the boundary of AdS

$$X^\mu(\sigma, \sigma_2) = (\sigma_2, 0, 0, 0) \qquad Y^i(\sigma, \sigma_2) = \sigma\, \theta^i \tag{3.1}$$

The induced metric on the worldsheet is $\mathrm{d}s^2 = \sigma^{-2}\left(\mathrm{d}\sigma^2 + \mathrm{d}\sigma_2^2\right)$ that is, the worldsheet describes an AdS_2 subspace of AdS_5, with area element $\mathrm{d}^2\sigma = \frac{1}{\sigma^2}\mathrm{d}\sigma\mathrm{d}\sigma_2$. The area swept by this string is divergent and need to be regularized. Setting a cut-off at $\sigma = \varepsilon > 0$ we get

$$A = \frac{L}{\varepsilon}$$

where L is the (infinite) length of the line. The regularized area is then zero and the Wilson loop as a trivial expectation value

$$\langle W \rangle = 1$$

This was expected since the straight line is a 1/2 BPS operator and it falls in the class of protected operators studied by Zarembo [9].

3.1.2. CIRLE

We parametrize the circle by

$$x^\mu(\sigma_2) = (a\cos\sigma_2, a\sin\sigma_2, 0, 0)$$

By means of special conformal transformations of the $SO(1,5)$ euclidean conformal group

$$x'^\mu = \frac{x^\mu + c^\mu(x^2+y^2)}{1+2c\cdot x + c^2(x^2+y^2)} \tag{3.2}$$

$$y' = \frac{y}{1+2c\cdot x + c^2(x^2+y^2)} \tag{3.3}$$

we can map a straight line $x^\mu(\sigma_2) = (\sigma_2, a/2, 0, 0)$ into the circle by taking $c^\mu = (0, -1/2a, 0, 0)$.

By the same transformation, the half-plane ending on the straight line is mapped to the hemisphere

$$x_1^2 + x_2^2 + y^2 = a^2$$

ending on the circle of radius a. The metric induced on the worldsheet becomes

$$\mathrm{d}s^2 = \frac{a^2}{y^2(a^2-y^2)}\mathrm{d}y^2 + \frac{a^2-y^2}{y^2}\mathrm{d}\phi^2$$

where ϕ is the angular polar coordinate $x_1 = a\cos\phi$, $x_2 = a\sin\phi$.

The area element is $\mathrm{d}^2\sigma = a\, y^{-2}\mathrm{d}y\mathrm{d}\phi$, then the area is

$$A = 2\pi\left(\frac{1}{\varepsilon} - 1\right)$$

and the expectation value of the Wilson loop, after the regularization, is

$$\langle W\rangle = e^{\sqrt{\lambda}}.$$

This result is surprising: since the circle and the straight line are related by a conformal transformation, we would expect they should have the same expectation value. However, the regularization breaks conformal invariance and the different expectation values are the effect of the conformal anomaly. In particular, the conformal transformation we used is changing the cut-off prescription for the regularization.

Moreover, the conformal transformation that maps the straight line onto the circle is a large conformal transformation and it is not a symmetry of $\mathbb{R}^4$, since it maps the point at the infinity to a point at finite distance and viceversa. Therefore it is a proper symmetry only for the theory compactified on S^4. As we saw in section 2.4, it is possible to relate the expectation value of the circle exactly to the fluctuation of the fields at the point at infinity.

3.1.3. Antiparallel lines

Another important configuration are the antiparallel lines. This is the case where the physical interpretation of the expectation value of the Wilson loop is more straightforward.

Since a Wilson line is the phase factor associated to the propagation of a massive quark in the fundamental representation of the gauge group, we can relate its expectation value to the effective static potential between an infinitely massive quark-antiquark pair. We think to the antiparallel line as a degenerate rectangle $L \times T$ where the temporal dimension T is infinitely extended. The potential between a quark-antiquark pair at a distance L is then given by

$$V(L) = \lim_{T\to\infty} -\frac{1}{T}\log\langle W(\mathcal{C})\rangle$$

If we take the two lines to have the same coupling to the scalar, that is the worldsheet lies on a fixed point on S^5, we have [12][30]

$$\langle W(\mathcal{C})\rangle = \exp\left(\frac{4\pi^2\sqrt{\lambda}}{\Gamma(1/4)}\frac{T}{L}\right)$$

which corresponds to a potential

$$V(L) = \frac{4\pi^2}{\Gamma(1/4)}\frac{\sqrt{\lambda}}{L}$$

The dependence on $1/L$ is the one expected, since the theory is conformal, hence $\langle W(\mathcal{C})\rangle$ can only be a function of T/L. In this configuration, the system is not supersymmetric, so that the supersymmetry does not protect our observable from radiative corrections. In fact, at strong coupling the effective Coulomb charge turns out to be proportional to $\sqrt{\lambda}$, while at weak coupling it is proportional to λ. This is a screening effect due to the resummation of all planar Feynman diagrams.

If we take the two lines to lie on antipodal points on the S^5, the system turns out to be supersymmetric. The Wilson loop has a trivial expectation value $\langle W(\mathcal{C})\rangle = 1$ since it's protected by supersymmetry and it falls into the Zarembo class. The worldsheet configuration is that of two parallel planes extending in the interior of AdS and ending on the two lines. As we will see, this is similar to the case of two circle along an Hopf fibration, when the scalar coupling makes the system BPS.

3.1.4. 1/4 BPS circular loop

If we consider a circular Wilson loop coupling to three scalar fields, rather than only to one scalar field, the operator preserves in general 1/4 of the

supersymmetry[31]. This system is a particular case of the DGRT loops presented in section 2.3.

In (2.1), let us consider the scalar couplings

$$\Theta^1 = \sin\theta_0 \cos\sigma_2 \qquad \Theta^2 = \sin\theta_0 \sin\sigma_2 \qquad \Theta_3 = \cos\theta_0 \tag{3.4}$$

with an arbitrary fixed θ_0.

Evaluating this operator at strong coupling requires finding a surface that partially wraps an $S^2 \subset S^5$ and is contained in a $AdS_4 \times S^2$ subset of $AdS_5 \times S^5$, We take the target space metric

$$ds^2 = -\cosh^2\rho d\tau^2 + d\rho^2 + \sinh^2\rho d\psi^2 + d\theta^2 + \sin^2\theta d\phi^2$$

where (θ, ϕ) describes the S^2.

We make the following ansatz in order to find the minimal area surface

$$\rho = \rho(\sigma) \qquad \psi(\sigma_2) = \sigma_2 \qquad \theta = \theta(\sigma_2) \qquad \phi(\sigma_2) = \sigma_2 \qquad \tau = 0 \tag{3.5}$$

The action functional in conformal gauge, where $\sqrt{h}h^{ab} = \delta^{ab}$, is

$$S = \frac{\sqrt{\lambda}}{4\pi} \int d^2\sigma \left(\rho'^2 + \sinh^2\rho + \theta'^2 + \sin^2\theta\right)$$

We find the equations of motion and the Virasoro constraint

$$\rho'' = \sinh\rho\cosh\rho \tag{3.6}$$

$$\theta'' = \sin\theta\cos\theta \tag{3.7}$$

$$\rho'^2 + \theta'^2 = \sinh^2\rho + \sin^2\theta. \tag{3.8}$$

We can decompose the Virasoro constraint in the AdS and S part since the motions are independent and (3.8) can only be satisfied if

$$\rho'^2 - \sinh^2\rho = c$$

If we take $c \neq 0$, the surface would start at the boundary of AdS, reach a minimum in the bulk and come back to a different point on the boundary: this configuration corresponds to the correlator of two different loops and we will study a similar configuration in the following.

We set $c = 0$, in order to obtain the surface corresponding to a single circle. Then we find

$$\sinh\rho = \frac{1}{\sinh\sigma}$$

where the integration constant, that would shift σ has been reabsorbed by worldsheet reparametrization invariance.

The first integral for θ is now

$$\theta'^2 = \sin^2\theta$$

and is solved by

$$\sin\theta = \frac{1}{\cosh(\sigma_0 \pm \sigma)}$$

where the starting point is fixed by the boundary condition $\theta(\sigma = 0) = \theta_0$. Depending on the sign, we found two surfaces wrapping over the north or south pole of the S^2 and only one will be dominant.

We can finally evaluate the action of these solutions

$$S = \sqrt{\lambda}\int \mathrm{d}\sigma(\sinh^2\rho + \sin^2\theta) = \sqrt{\lambda}(\cosh\rho_{\mathrm{Max}} \mp \cos\theta_0)$$

where ρ_{Max} is a cut-off which regularize the integral.

The final regularized result is then

$$S = \mp\cos\theta_0\sqrt{\lambda}$$

where the sign must be choosen to minimize the action and the corresponding expectation value of the Wilson loop at strong coupling is

$$\langle W(\mathcal{C})\rangle = \exp\left(\pm\cos\theta_0\sqrt{\lambda}\right).$$

This results is quite interesting, since by varing θ_0, it allows to interpolate between two known results with enhanced supersymmetry: if we take $\theta_0 = 0$ we fall back to the 1/2 BPS circular loop coupled to a single scalar field, while for $\theta_0 = \pi/2$ the loop fits the Zarembo construction of section 2.2 and has trivial expectation value.

The result also agrees with the perturbative computation. In that case the computation is very similar to the one for the 1/2 BPS loop, the only difference being a rescaling of the coupling constant $\lambda \to \lambda\cos^2\theta_0$. Therefore the agreement between weak and strong coupling computations holds even for this less supersymmetric configuration.

3.2. Systematic regularization

As it can be seen in the previous examples, the area of the worldsheet surface dual to the Wilson loop is always divergent. This is due to the AdS metric and to the request that the surface reaches the (conformal) boundary of AdS to end on the loop. Thus the result needs to be regularized.

It can be shown [32] that the divergent contribution comes from a small region near the boundary. If we consider a small cut-off $\epsilon > 0$ and the surface ending at $Y = \epsilon$ rather than at $Y = 0$, the divergent contribution to the area is

$$A = \frac{1}{\epsilon}\oint_{\mathcal{C}} \mathrm{d}\sigma^2|\dot{x}|$$

and it is proportional to the length of the loop itself.

In the original work of Maldacena [12], the divergence is associated to the infinite mass of the heavy W-boson associated to the open string stretching between the stack of N D3-branes where the $U(N)$ theory lives and the infinitely far away brane in the $U(N+1) \to U(N) \times U(1)$ symmetry breaking mechanism.

A systematical analysis of the problem reveals that one does not need any regularization, once we impose the correct boundary conditions. The loop variables $\dot{y}^I$ impose Neumann boundary conditions on the Y^I coordinates. Therefore the Wilson loop should be regarded as a functional of the X^μ coordinates and the momenta P_I conjugate to Y^I on the boundary

$$P_I = \frac{\delta A}{\delta \partial_1 Y^I} = \sqrt{h} h^{1a} G_{IJ} \partial_a Y^J$$

The Nambu-Goto action, that we used to compute the area, is a functional of the $X^\mu(\sigma^2)$ and $Y^I(\sigma^2)$ and it would be appropriate for full Dirichlet boundary conditions. We can define a functional tailored on our mixed boundary conditions by a Legendre transformation

$$\tilde{A} = A - \int \mathrm{d}^2\sigma \partial_1 (P_I Y^I) = A + \oint_{\mathcal{C}} \mathrm{d}\sigma^2 P_I Y^I$$

The Neumann boundary conditions

$$j_2{}^a \partial_a Y^I(0, \sigma^2) = \dot{y}^I(\sigma^2)$$

become Dirichlet conditions on the momenta

$$\dot{y}^I = P^I = Y^2 P_I$$

and the new functional differs from the old one exactly by a divergent term proportional to the length of the loop

$$\tilde{A} = A + \oint_{\mathcal{C}} \mathrm{d}\sigma^2 \frac{\dot{y}^I}{Y^2} \delta_{ij} Y^j = A - \frac{1}{\epsilon} \oint_{\mathcal{C}} \mathrm{d}\sigma^2 |\dot{y}|$$

where we set $Y = \epsilon$ and the condition (1.12), $|\dot{x}| = |\dot{y}|$, that is the requirement that the scalar couplings lie on a S^5, $\theta_I \theta_I = 1$ and the loop is locally supersymmetric, ensures the cancellation.

3.3. Ansatz and excited charges

Depending on the ansatz we make to reduce the equations of motion to a form we are able to solve, we can turn on different kind of conserved charges. Instead of trying to solve the most general ansatz, we will restrict ourself to some interesting subsets of the full $\mathrm{AdS}_5 \times S^5$ target space, following the spirit of [33].

We choose to analyze the specific set up of Hopf fibers, since this configuration seems to be a good candidate for the search of supersymmetric solutions. As soon has we move to the strong coupling dual however, the treatment of supersymmetry becomes highly nontrivial. A powerful tool, which greatly simplifies this problem, is the possibility to express the solutions in term of surfaces calibrated by almost complex structures (see 2.5).

As far as the DGRT construction is involved, we can restrict to an $AdS_4 \times S^2$ subspace of the target space, so that the almost complex structure can be built out by analogy with the almost complex structure on S^6.

In order to restrict our string solution to this subspace, in this work we will turn on three different type of charges:

- a angular momentum on AdS, which describes two loops ending on different Hopf fibers of the same fibration;

- a angular momentum on S, which describes loops with different scalar couplings

- the dilation charge, which relates loops with different radii and gives raise to a phase transition phenomenon.

A tricky feature of the correlator of Wilson loops we are studying is that the geometric data describing the system (the angular distance between different Hopf fibers, the angular distance on S^5 and the ratio of the radii) are not encoded in a straightforward manner in term of the first integrals of motion that we use to parametrize the solution. This quantities are usually expressed by means of non-trivial equations involving elliptic functions that cannot be inverted. Moreover, there is not a one-to-one correspondence between the parameters and the physical (geometric) quantities. The survey of the solutions is therefore quite involved and requires numerical analysis.

3.4. Hints of 1-loop computation

It would be interesting to take into account the first quantum corrections to our classical results.

To this aim, we need to compute the 1-loop corrections [34]. In particular we need to evaluate the 1-loop determinant Γ_1 that appears in the partition function. To do this, we need the spectra of the quadratic bosonic and fermionic fluctuations over the surface that correspond to the classical solution we are considering. For simple cases, it is possible to explicitly evaluate the eigenvalues spectrum by Gelfand-Yaglom methods [35][36] that express the determinant in terms of the solution of an initial value problem.

This is possible following the observation of [37][38] that fluctuations $f(x)$ on a class of solutions expressed in term of elliptic functions can be put

in a standard single-gap Lamé form

$$\left[-\partial_x^2 + V(x) - \Lambda\right] f(x) = \Lambda f(x).$$

The solution to this equation can be expressed in term of Jacobi Eta H, Theta Θ and Zeta Z functions. The two independent Bloch solutions are

$$f_\pm(x) = \frac{H(x \pm \alpha)}{\Theta(x)} e^{\mp x Z(\alpha)}$$

where the spectral parameter $\alpha = \alpha(\Lambda)$ depends on the eigenvalue Λ by the equation

$$\mathbf{sn}(\alpha|k) = \sqrt{\frac{1 + k^2 - \Lambda}{k^2}}.$$

By periodicity properties of Jacobi functions it is then possible to define the quasi-momenta

$$p(\Lambda) = iZ(\alpha|k) + \frac{\pi}{2\,\mathbf{K}(k)}$$

and we can express the determinant as

$$\det\left[-\partial_x^2 + 2k^2\,\mathbf{sn}^2(x|k)\right] = \begin{cases} -4\sin^2\left(\dfrac{L}{2}p(\Lambda)\right) & \text{periodic} \\ +4\cos^2\left(\dfrac{L}{2}p(\Lambda)\right) & \text{antiperiodic} \end{cases}$$

This corrections have already been computed for some of the elementary example we described so far. The correction to the straight line and the circle were computed in [39]. Since the result for the straight line was already known, being a BPS system, the computation was use as a test for the regularization prescription. The 1-loop computations can be regularized in a nice way by subtracting a reference solution. For the circular Wilson loop, the regularized 1-loop determinant gives

$$\Gamma_1 = \frac{1}{2}\ln 2\pi$$

in agreement with the gauge theory result.

In [40], the 1-loop corrections for the antiparallel lines were computed analitically and the first correction to the quark-antiquark potential turns out to be

$$V(L) = -\frac{\sqrt{\lambda}}{\pi L}\left(1 - \frac{\pi}{\sqrt{\lambda}} + \mathcal{O}\left(\frac{1}{\sqrt{\lambda}^2}\right)\right)$$

The result was then generalized to a whole 1-parameter family of loops, interpolating between the circle and the antiparallel lines in [41].

The configurations we will study in detail in chapter 4 are in some sense similar to this construction. We can always express our solutions in terms

of elliptic functions and in a particular limit we can find back the system of antiparallel lines. Our ansatz is a different generalization of the antiparallel lines and it would be interesting to compute the 1-loop determinant in that case.

Chapter 4

Hopf fibers correlators

We will now compute the correlator of two Wilson loops living on two Hopf fibers at strong coupling and analyze some particular limits with important physical interpretations. Part of the results presented here have already been published [42], while the more recent ones will appear in a paper in preparation.

4.1. Strong coupling solution

We work in global coordinates (1.1) and in conformal gauge, which means that the worldsheet metric obeys $\sqrt{\gamma}\gamma^{ab} = \delta^{ab}$ with Euclidean signature. In order to guarantee the diffeomorphism invariance of the worldsheet, we must impose Virasoro constraints on the energy-momentum tensor

$$T_{ab} = \left(\partial_a X^M \partial_b X^N - \frac{1}{2}\gamma_{ab}\gamma^{cd}\partial_c X^M \partial_d X^N\right) G_{MN} = 0.$$

These can be expressed in term of the induced metric on the worldsheet

$$h_{ab} = G_{MN}(X)\partial_a X^M \partial_b X^N$$

as

$$\begin{aligned} T_{11} &= -T_{22} = \tfrac{1}{2}(h_{11} - h_{22}) = 0 \\ T_{12} &= h_{12} = 0 \end{aligned}$$

Thanks to the product geometry of the target space, we can choose coordinates where G_{MN} is diagonal with respect to the factor spaces

$$G_{MN}(X) = \begin{pmatrix} G^{\mathrm{AdS}_5}_{mn}(x) & 0 \\ 0 & G^{S^5}_{IJ}(\Theta) \end{pmatrix}$$

Thus, we can separate the contribution to the energy-momentum tensor and to the action coming from each factor, ending up with two distinct σ-models

$$S = S_{\mathrm{AdS}_5} + S_{S^5}.$$

$$\mathcal{L}^{\mathrm{AdS}} = h_{11}^{\mathrm{AdS}} + h_{22}^{\mathrm{AdS}} \qquad\qquad \mathcal{L}^{S^5} = h_{11}^{S^5} + h_{22}^{S^5}$$

The two models are still interacting through the Virasoro constraints

$$T_{ab} = T_{ab}^{\mathrm{AdS}_5} + T_{ab}^{S^5}$$

and they share the same worldsheet coordinates (σ, σ_2), so we will need to impose the boundary condition in such a way to match the ranges of variation.

4.1.1. S^5 MOTION

As far as DGRT loops are concerned, we can restrict the motion in a $S^2 \subset S^5$, by setting $\Theta^4 = \Theta^5 = \Theta^6 = 0$.

The relevant coordinates are then

$$\Theta^1 = \cos\alpha \sin\beta \qquad \Theta^2 = \sin\alpha \sin\beta \qquad \Theta^1 = \cos\beta$$

and the metric is

$$G_{S^2} = \begin{pmatrix} 1 & \\ & \sin^2\beta \end{pmatrix}.$$

The induced metric is

$$\begin{aligned} h^S_{\sigma\sigma} &= \beta'^2 + \sin^2\beta \alpha'^2 \\ h^S_{\sigma_2\sigma_2} &= \dot\beta^2 + \sin^2\beta \dot\alpha^2 \\ h^S_{\sigma\sigma_2} &= \dot\beta\beta' + \sin^2\beta\, \dot\alpha\alpha' \end{aligned}$$

For loops in an Hopf fibration, the scalar couplings are fixed by the DGRT construction to

$$\sigma_1^{(R)} = \sigma_2^{(R)} = 0 \qquad\qquad \sigma_3^{(R)} = \mathrm{d}\psi = k\mathrm{d}\sigma_2$$

For parallel fibers, in order to have a supersymmetric configuration, the surface must sit entirely at one point in S^5. In this case, the motion is trivially solved by constant values of β and α.

If we consider antiparallel fibers, we need the two fibers to lie at antipodal points on S^5. The surface then must move along S^5 to connect the two points. We consider the simplest case, where the motion on S^5 is geodesic. Without loss of generality we can set

$$\beta(\sigma) = \beta_0 + J\sigma \qquad\qquad \alpha(\sigma) = \alpha_0$$

where α_0 and β_0 are constants determining the boundary conditions on the S^5 angles.

Finally, we have to consider the Virasoro constraints from the S^5 part. The off-diagonal part of the energy-momentum tensor vanishes identically because of the choice of geodesic motion

$$T_{12}^{S^5} = 0$$

The first Virasoro constraint instead gives

$$T_{11}^{S^5} = -T_{22}^{S^5} = \frac{1}{2}J^2.$$

4.1.2. AdS_5 MOTION

In global AdS coordinates, we make the following ansatz to solve the equations of motion [33]

$$\begin{aligned} &\rho = \rho(\sigma) && \tau = \tau(\sigma) \\ &\theta = \theta(\sigma) && \varphi = \varphi(\sigma) \\ &\psi = k\sigma_2 + \eta(\sigma) \end{aligned} \tag{4.1}$$

This means that we are choosing the coordinate $\sigma_2 \in [0, 4\pi)$ to parametrize the loop.

With this choice, the Lagrangian becomes

$$\mathcal{L}^{\text{AdS}} = \rho'^2 + \cosh^2\rho\ \tau'^2 + \frac{1}{4}\sinh^2\rho\left(\theta'^2 + \varphi'^2 + \eta'^2 + 2\cos\theta\ \varphi'\eta' + k^2\right)$$

Since the Lagrangian does not depend on τ, φ and η we have three first integrals of motion

$$\cosh^2\rho\ \tau' = \frac{t}{2} \tag{4.2}$$

$$\sinh^2\rho\ (\varphi' + \cos\theta\,\eta') = c_\varphi \tag{4.3}$$

$$\sinh^2\rho\ (\eta' + \cos\theta\,\varphi') = c_\eta \tag{4.4}$$

The Virasoro constraints for the AdS part becomes

$$T_{12}^{AdS} = k(\eta' + \cos\theta\varphi') = 0 \tag{4.5}$$

$$T_{11}^{AdS} = \frac{1}{2}\left(\rho'^2 + \cosh^2\rho\,\tau'^2 + \sinh^2\rho\left(|v'|^2 - \dot{\psi}^2\right)\right) = -\frac{1}{2}J^2 \tag{4.6}$$

where we collected the coordinates describing the Hopf fibration in a vector

$$v = (\theta, \varphi, \eta)$$

We can see that the equations of motion and the second Virasoro constraint single out a geodesic motion on the S^3 in the parametrization

$$|v'|_{S^3} = \frac{c_v}{\sinh^2\rho}. \tag{4.7}$$

In fact[1],

$$v''^m + \Gamma^m_{nk} v'^n v'^k = v'^m \partial_\sigma \ln \frac{1}{\sinh^2 \rho}$$

Moreover, from the second Virasoro constraint $T^{\mathrm{AdS}}_{12} = 0$ we have

$$\frac{k}{2} \sinh^2 \rho \, (\eta' + \cos\theta \, \varphi') = 0.$$

so the η-equation (4.4) is satisfied for $c_\eta = 0$. The equation then allows to express the dynamics only in term of the angles on the S^2 base of the Hopf fibration

$$\eta' + \cos\theta \, \varphi' = 0.$$

Actually, only one angle is dynamically independent. From (4.3) and (4.7) we find in fact

$$\theta'^2 = \frac{c_v^2}{\sin^2\theta \sinh^4\rho} \left(\sin^2\theta - \frac{c_\varphi^2}{c_v^2} \right)$$

and the motion on the base S^2 is geodesic.

Since our ansatz singles out geodesic motion, we can without loss of generality choose our coordinates system in such a way that the ψ angle is independent of σ and the motion on the S^2 base is along a great circle. We rephrase the ansatz in order to simplify the notation in the following way

$$\begin{aligned} \psi &= k\sigma_2 \\ \theta &= \theta(\sigma) \\ \phi &= \phi_0 \end{aligned}$$

In this way, the equations of motion for ϕ and ψ and the second Virasoro constraint are trivially satisfied.

With this choice of coordinates, the first Virasoro constraint now reads

$$\rho'^2 + \cosh^2\rho \, \tau'^2 + \sinh^2\rho (\theta'^2 - k^2) = -J^2 \tag{4.8}$$

The remaining first integrals (4.2) and (4.3) are

$$\tau' = \frac{kt}{2\cosh^2\rho} \qquad\qquad \theta' = \frac{kp}{\sinh^2\rho} \tag{4.9}$$

and finally the equation of motion for ρ is

$$\rho'' = \sinh\rho\cosh\rho \left(\frac{k^2}{4} - \tau'^2 - \frac{\theta'^2}{4} \right) \tag{4.10}$$

[1]For the 3-sphere we have $\Gamma^\varphi_{\theta\varphi}(S^3) = \Gamma^\psi_{\theta\psi}(S^3) = \frac{1}{2}\frac{\cos\theta}{\sin\theta}$, $\Gamma^\varphi_{\theta\psi}(S^3) = \Gamma^\psi_{\theta\varphi}(S^3) = -\frac{1}{2\sin\theta}$, $\Gamma^\theta_{\varphi\psi}(S^3) = \frac{1}{2}\sin\theta$

4.1.3. Boundary conditions

The boundary conditions of the worldsheet are fixed by the presence of the loops at the boundary of AdS.

The Hopf fiber loops lie along the ψ direction. Hence, we need to provide boundary conditions for the other coordinates as the worldsheet reaches the boundary, that is $\rho \to \infty$. By worldsheet reparametrization invariance, we can always take the first boundary to be at $\sigma = 0$. Then the solution to the ρ equation will fix the other boundary $\Delta\sigma$ when ρ comes back to the infinity. We then must impose

$$\theta(0) = \theta_1 \qquad \theta(\Delta\sigma) = \theta_2 \tag{4.11}$$

$$\tau(0) = \tau_1 \qquad \tau(\Delta\sigma) = \tau_2 \tag{4.12}$$

$$\beta(0) = \beta_1 \qquad \beta(\Delta\sigma) = \beta_2 \tag{4.13}$$

where θ_1 and θ_2 are the base points of the two fibers, β_1 and β_2 define the scalar couplings and $\exp(\tau_1)$ and $\exp(\tau_2)$ are the radii of the 3-spheres where the fibers lie.

4.1.4. Solutions to the equations of motion

We start noticing that the ρ-equation (4.10) and the Virasoro constraint (4.8) are compatible: in fact, differentiating the Virasoro constraint with respect to σ gives precisely the equation of motion. It is then sufficient to find a solution to the Virasoro constraint and this will automatically be a solution to the equation of motion. This is a great simplification, since the Virasoro constraint is a first order (although nonlinear) differential equation, while the equation of motion is a second order differential equation.

Inserting the first integrals (4.9) in the first Virasoro constraint (4.8) we are able to decouple the equation for the radial variable ρ:

$$\rho'^2 = \frac{k^2}{4}\left(\sinh^2\rho - \frac{t^2}{\cosh^2\rho} - \frac{p^2}{\sinh^2\rho}\right) - J^2.$$

Setting $\sinh\rho = R$, the equation becomes

$$R'^2 = \frac{k^2}{4}\left(R^4 + (1-\alpha^2)R^2 - (\alpha^2 + t^2 + p^2) - \frac{p^2}{R^2}\right)$$

where $\alpha = \frac{2J}{k}$, and it can be integrated as

$$\frac{k\sigma}{2} = \int_R^\infty \frac{R\,\mathrm{d}R}{(R^6 + (1-\alpha^2)R^4 - (\alpha^2 + t^2 + p^2)R^2 - p^2)^{\frac{1}{2}}}$$

This integral can be solved in term of elliptic functions (Appendix D)

$$R^2 = \frac{A}{\mathbf{sn}^2\left(\frac{k\sqrt{A}\sigma}{2}, l\right)} - B \tag{4.14}$$

where A, B and l are constants that depend in a nontrivial way on the integration parameters α, t and p. For further discussions, we note that the total range of variation of the worldsheet coordinate is $\Delta\sigma = \frac{4}{k\sqrt{A}}\,\mathbf{K}(l)$, which is the value where the surface goes back to the boundary of AdS.

Given the solution, we can compute the area swept by the surface from the Nambu-Goto action

$$\begin{aligned}\frac{\text{Area}}{\sqrt{\lambda}} &= \int \mathrm{d}^2\sigma\sqrt{h} = \\ &= A^{-\frac{1}{2}}\left((A-B)\,\mathbf{K}(l) - A\,\mathbf{E}(l)\right)\end{aligned} \tag{4.15}$$

and the other physical quantities describing the system from (4.9)

$$\Delta\theta = \frac{4p}{\sqrt{A}B}\left(\mathbf{\Pi}\left(\frac{B}{A},l\right) - \mathbf{K}(l)\right) \tag{4.16}$$

$$\Delta\tau = \frac{2t}{\sqrt{A}(B-1)}\left(\mathbf{\Pi}\left(\frac{B-1}{A},l\right) - \mathbf{K}(l)\right) \tag{4.17}$$

$$\Delta\beta = \frac{2\alpha}{\sqrt{A}}\,\mathbf{K}(l) \tag{4.18}$$

4.2. Discussion of results

We will discuss our results in some particular limits, namely taking some of the parameters to vanish. This strategy has a double purpose. On one hand, it is sometimes possible to give a more explicit form for the solution, making the result clearer. On the other hand we find some configurations that are already present in the literature, but in different coordinate systems. This allows us to check the correctness of our derivation.

After checking the matching with known results, we will analyze the emergence of a phase transition phenomenon and enlight the characteristic of the phase space, starting from simplified configurations, where an actual visualization of the solution is possible, to arrive at the most general one.

Finally, we will focus on a specific configuration, where the loops are in an "almost flat" limit and we can interpret the results in terms of static potential for a quark-antiquark pair.

4.2.1. Coincident circles with different scalar couplings

If we take $p = t = 0$, the two loops are in the same point on the same S^2 base of the Hopf fibration. Since $\alpha \neq 0$ however, their couplings with the scalar field are different.

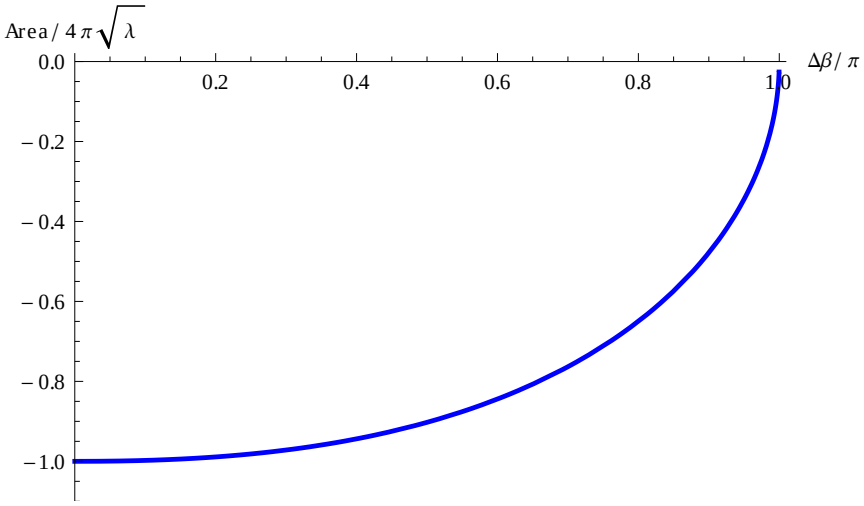

FIGURE 4.1: The area of coincident loops with different scalar couplings increases with the angular separation on the S^5. The supersymmetric case, for $\Delta\beta = \pi$ has trivial expectation value Area= 0.

In this case the solution is

$$R^2 = \frac{1}{\mathbf{sn}^2\left(\frac{k(1+\alpha^2)^{1/2}\sigma}{2}, \frac{1}{1+\alpha^2}\right)} - 1$$

and the surface of the area and the angular distance on S^5 are

$$\text{Area} = \frac{4\pi}{(1+\alpha^2)}\left(\alpha^2\,\mathbf{K}\left(\frac{1}{1+\alpha^2}\right) - (1+\alpha^2)\,\mathbf{E}\left(\frac{1}{1+\alpha^2}\right)\right) \tag{4.19}$$

$$\Delta\beta = \frac{2\alpha}{(1+\alpha^2)^{\frac{1}{2}}}\,\mathbf{K}\left(\frac{1}{1+\alpha^2}\right) \tag{4.20}$$

We check that, as expected, increasing the angular separation on S^5 the surface of the area increases. In the case of antipodal points, $\Delta\beta = \pi$, the configuration is supersymmetric and we find the correct vanishing area, so that the expectation value of the Wilson loop is trivial $\langle W \rangle = 1$.

4.2.2. Coplanar loops of different radii

If we take the limit of $\alpha = p = 0$ while $t \neq 0$, the two loops are coplanar concentric circles with the same coupling to the scalar. The solution to the equations of motion is (4.14) with parameters

$$B = 0 \qquad A = \frac{1}{2}\left(\sqrt{1+4t^2} - 1\right) \qquad l = -\frac{1+2t^2+\sqrt{1+4t^2}}{2t^2} \tag{4.21}$$

and the ratio between the radii is the exponential of (4.17).

Since we have two loops of different dimensions, within the class of DGRT loops, the supersymmetry is broken by the length scale introduced by the scalar couplings. This will be true for all the configurations with $t \neq 0$. Nevertheless, this configuration is quite interesting.

This layout was studied by Gross and Ooguri [43] (see also [44]) in a different coordinate system. The most striking feature is the appearance of a phase transition in the behavior of the area as a function of the ratio of the radii of the circles.

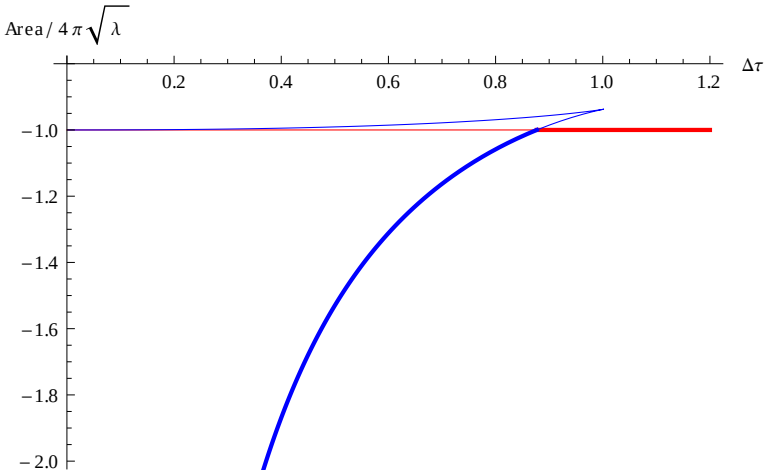

FIGURE 4.2: Gross-Ooguri phase transition: until the radii of the loop are similar, the connected surface dominates (blue thick line); when the ratio is grater than the critical point, $\frac{R_f}{R_i} = 2.40343$, the disconnected surface dominates (red thick line). Further increasing the ratio, the string connecting the two fibers breaks and the connected solution ceases to exist. The breaking point is at $\frac{R_f}{R_i} = 2.7245$

.

We see that our result exactly reproduces the results of [43] and [24]. In fact, from figure 4.2, we see that until the quotient of radii is below $R_f/R_i = 2.7245$ two class of solutions exist: two connected solutions joining the two loops and a disconnected one where each loop has its own surface. Above this critical point instead, the string joining the loops breaks and only the disconnected solution survives.

In the region where both types of solutions exist, we need to determine which is dominant. In the large λ limit, only the solution with minimal area will contribute, since any other contribution would be exponentially suppressed. For $R_f/R_i < 2.40343$ one of the connected solution has minimal area, hence it is the relevant one for the expectation value of the correlator.

In this phase, the expectation value depends on the ratio of the radii of the two loops and increases with the ratio R_f/R_i. At the critical point, a first order phase transition takes place and the disconnected solution becomes dominant. Within this region the expectation value of the correlator is constant and it does not depend on the ratio of the radii.

This is a check of the validity of our results. The set up in Hopf fibration will allow to generalize this result to more general configurations, where the loops are not required to lie on the same plane, as we will see in the following.

4.2.3. Fibers with equal radius and scalar coupling

If we take $\alpha = t = 0$ and $p \neq 0$, we have two fibers located at different points on the S^2 base of the Hopf fibration with the same radius and the same coupling with the scalar.

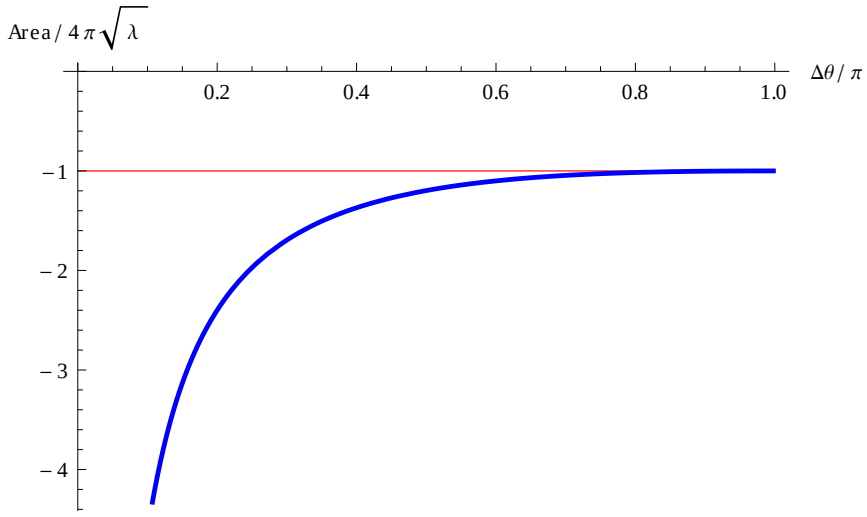

Figure 4.3: The area as a function of the angular separation of the two fibers on the S^2 basis of the Hopf fibration.

The solution is

$$R^2 = \frac{1+p}{\mathbf{sn}^2\left(\frac{k\sqrt{1+p}\sigma}{2}, \frac{1-p}{1+p}\right)} - 1 \tag{4.22}$$

with a total worldsheet coordinate range

$$\Delta\sigma = \frac{4}{k\sqrt{1+p}}\,\mathbf{K}\left(\frac{1-p}{1+p}\right)$$

The area and the angular distance between the fibers can be expressed

in terms of elliptic integrals

$$\text{Area} = \frac{4k\pi}{\sqrt{1+p}}\left(p\,\mathbf{K}\left(\frac{1-p}{1+p}\right) - (1+p)\,\mathbf{E}\left(\frac{1-p}{1+p}\right)\right)$$
$$\Delta\theta = \frac{4p}{\sqrt{1+p}}\left(\mathbf{\Pi}\left(\frac{1}{p+1}, \frac{1-p}{1+p}\right) - \mathbf{K}\left(\frac{1-p}{1+p}\right)\right)$$

and the dependence of the area on the angular separation is shown in figure 4.3. We can see that the connected solution has always area smaller than the disconnected one.

For $p \neq 0$, the system is not describing the connected correlator of two supersymmetric DGRT Hopf fibers. The non-supersymmetric nature of the connected solution is due to the opposite orientations of the two boundary circles. For Hopf fibers parametrized by $\psi = k\sigma_2$, the Wilson loop operator (2.7) becomes

$$W = \operatorname{Tr}\mathcal{P}\exp\int_0^{4\pi} \mathrm{d}t\,(i\dot{x}^\mu A_\mu + k\Phi_3)$$

because, for constant (θ, φ),

$$\theta^I = \operatorname{sign}(k)\delta^I_3.$$

When we consider the correlator $\langle W_1 W_2\rangle$ of two Hopf fibers, the configuration is BPS if the fiber have equally orientation with the same scalar coupling or opposite orientation with opposite (antipodal points on S^5) scalar couplings. On the contrary, our connected solution describes two opposite oriented fibers with the same scalar coupling, hence it represents a non supersymmetric configuration.

This can be explained in the following way. The string has no motion along S^5, implying that the fibers have the same scalar coupling. However, the orientation of the worldsheet, namely the tangential ∂_2 and "radial" ∂_1 direction, must be preserved. Since the surface has a turning point in the ρ target space coordinate, the sign of the radial direction is reversed on the two branches of the surface and the tangential direction must be reversed in order to preserve the orientation. The final picture is that of two antiparallel Hopf fibers with the same scalar charge.

In the $p \to 0$ limit, the separation between the two fibers is maximal $\Delta\theta \to \pi$ and the connected surface has the same area of the disconnected one. In this case, the two fibers lie on two planes along completely orthogonal directions: the first loop is in the $x_3 = x_4 = 0$ plane, while the second one is in the $x_1 = x_2 = 0$ plane. The system in this configuration turns out to be supersymmetric. In fact, each loop preserves half of the supersymmetry and the presence of the other one in the completely orthogonal plane halves the components of the independent supersymmetric spinors by imposing a chirality condition. The explicit computation can be found in [7]. There the

computation is performed in the case of parallel fibers, but in the special case of $\Delta\theta = \pi$ the result becomes insensible to the orientation, hence it applies also in the case of antiparallel loops that we are considering, which turns out to be 1/4 BPS.

Therefore, depending on p, our solution interpolates between non-BPS configuration $p \neq 0$ and a BPS one $p \to 0$.

The non supersymmetric nature of the connected solution can also be recognized at strong coupling from pseudo-holomophicity equations. Inserting the solution (4.22) into the Cauchy-Riemann equations (2.25) we get the constraints

$$\begin{array}{ccc} & \rho' + k\ \sinh\rho = 0 & \\ \theta' = 0 \qquad & \varphi' = 0 & \qquad \psi' = 0. \\ & \eta' + \cos\theta\ \varphi' = 0 & \end{array}$$

where we recognize the second Virasoro constraint and the other equations select the disconnected solution.

The existence of a connected solution for a supersymmetric configuration would spoil the conjecture that these systems are captured by a matrix model at any coupling (as described in section 2.4). In fact, the matrix model relies on the vanishing of the sum of all interacting Feynman diagrams, while the stringy effects due to the presence of a connected solution would spoil this picture. The fact that such a solution does not exist is a strong argument in favor of the conjecture, although this is not a proof, since the solution could exist for a more general ansatz. Our choice however is the most natural and we expect this result to hold in general.

4.2.4. Fibers with equal radius and different scalar couplings

If we take $t = 0$ and both $\alpha, p \neq 0$, we are considering fibers lying on different points of the S^2 base of the Hopf fibration and with different scalar couplings.

This layout can be interesting, since we may be able to find a connected solution for a BPS configuration: if we are able to find a solution that ends at antipodal point on S^5, the fibers will be antiparallel and with opposite scalar couplings, hence the configuration would be supersymmetric. However, we will find that within our ansatz such a solution does not exists.

In this case the solution is again (4.14) with parameters

$$B = 1 \qquad A = \frac{1}{2}\left(2 + \alpha^2 + \sqrt{\alpha^4 + 4p^2}\right)$$
$$l = \frac{2(1 + \alpha^2 - p^2)}{2 + 2(\alpha^2 + p^2) + \alpha^4 + (2 + \alpha^2)\sqrt{\alpha^4 + 4p^2}}$$

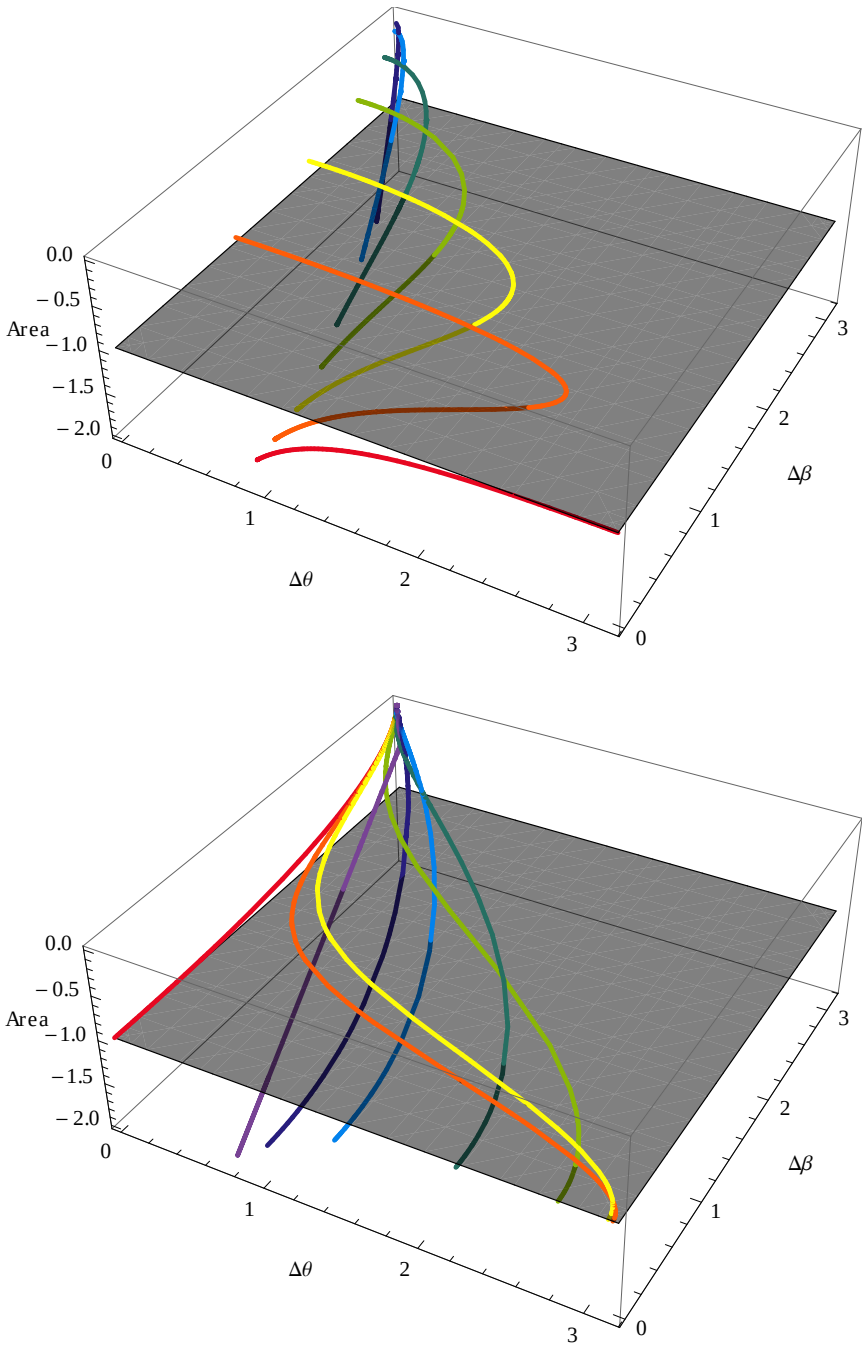

FIGURE 4.4: The area of the solutions at constant α (above) and p (below) as a function of the angular separations $\Delta\theta$ and $\Delta\beta$

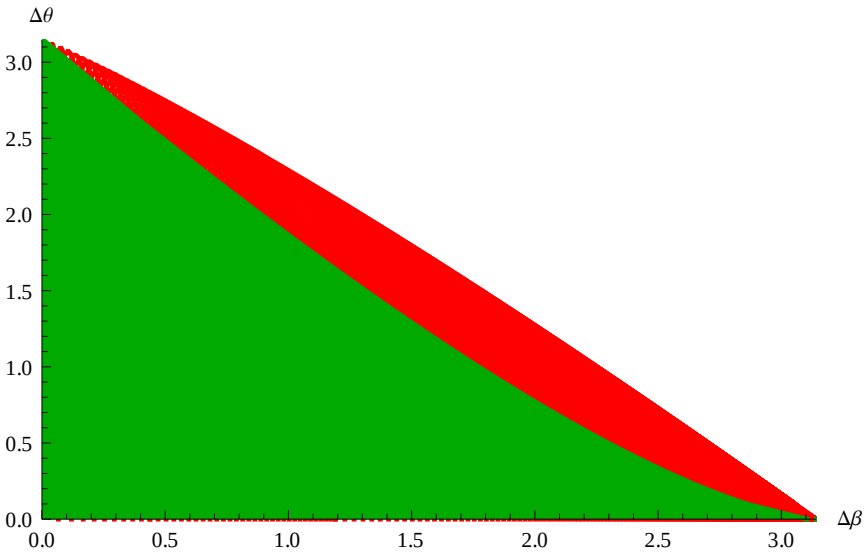

FIGURE 4.5: The phase diagram over $\Delta\theta$ and $\Delta\beta$: for small separations the connected solution dominates (green). Increasing the separation the connected solution becomes subleading (red) with respect to the disconnected one and eventually disappears at all (white). For supersymmetric configurations, that is $\Delta\beta = \pi$ (opposite scalar couplings) or $\Delta\theta = \pi$ (fibers on orthogonal planes), the only solution is the disconnected one.

In figure 4.4, we can see the dependence of the area with respect to $\Delta\theta$ and $\Delta\beta$, for constant α and p. We stress out the nontrivial dependence of the angles on the integration parameters α and p.

From figure 4.5 we see that there are two different phases. For small angular separation, the connected solution is dominant. Increasing the angular separation, both in the θ and in the β direction, the disconnected solution becomes dominant.

It is possible to have supersymmetric configuration in two different limits. In the first one, when $\Delta\beta = \pi$, the two fibers have opposite scalar couplings and orientation. In the second one, when $\Delta\theta = \pi$, the two fibers lies on completely orthogonal planes. If we fix for instance $\theta_1 = 0$, the first loop lies on the $(0, 0, x_3, x_4)$ plane while the other one, at $\theta = \pi$ lies on the plane $(x_1, x_2, 0, 0)$.

We see from the phase diagram that in these limits the only solution is the disconnected one.

Also in this case, as for 4.2.3, it is possible to check that imposing the pseudo-holomophicity of the surface singles out the disconnected solution, while the connected solution breaks supersymmetry.

A similar setup was studied in [45], where it was shown that pseudo-holomorphic minimal surfaces only exist in a $AdS_3 \times S^2$ subset of the target space if the Virasoro constraint are separately satisfied on AdS, $T^{AdS}_{\alpha\beta} = 0$, and on S, $T^{S}_{\alpha\beta} = 0$. Imposing this condition on our configuration selects the $\alpha = 0$ and then we fall back to the previous case.

As already discussed in 4.2.3, this is a strong argument, although not a final proof, in support to the hypothesis that BPS configuration are captured by the matrix model 2.4. This result further extend the range of validity of the conjecture.

We will further analyze this configuration in the almost flat limit $\Delta\theta \to 0$, where it is possible to relate the result to the static quark-antiquark potential, in section 4.4.

4.2.5. Fibers with different radii

If we take $p \neq 0$ and $t \neq 0$, while keeping $\alpha = 0$, we are considering the correlator of two Hopf fibers with the same scalar coupling but different radii. This is a generalization of the configuration studied in 4.2.2: here the two loops lie on different planes.

Since the radii are different, the supersymmetry is broken by DGRT construction. The situation is qualitatively similar to the case when $p = 0$. However, increasing the separation between the fibers, the region where the connected solution dominates becomes narrower. When we reach the configuration where the two loops lie on completely orthogonal planes $(x_1, x_2, 0, 0)$ and $(0, 0, x_3, x_4)$, that corresponds to $\Delta\theta = \pi$, the only solution is the disconnected one for any ratio of the radii.

4.2.6. Coplanar fibers with different radii and scalar couplings

If we take $\alpha \neq 0$ and $t \neq 0$, while $p = 0$, the two fibers lie on the same plane (e.g. $x_3 = x_4 = 0$) but have different radii and different scalar couplings.

Increasing the difference of scalar couplings, the range of radii where the connected solution exists becomes narrower. When the loops are at antipodal point, $\Delta\beta = \pi$, again the connected solution does not exist for any ratio of the radii, even if the supersymmetry is broken by the DGRT construction.

4.2.7. General case

Collecting all the results from the previous particular cases, we are able to give a general picture of the phase space for generic parameters.

The correlator of two Wilson loops over Hopf fibers is described by two

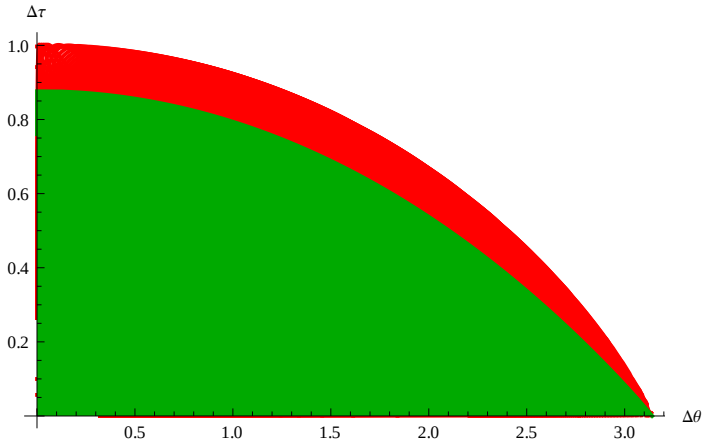

FIGURE 4.6: The phase diagram over $\Delta\theta$ and $\Delta\tau$: for small $\Delta\theta$ and $\Delta\tau$ the connected solution dominates (green area). Increasing the ratio of the radii, the disconnected solution becomes dominant (red area). Further increasing the separation, the connected solution ceases to exist (white area) and the string connecting the two loops breaks. The region where the connected solution is dominant becomes narrower as the angular separation between the fibers increases.

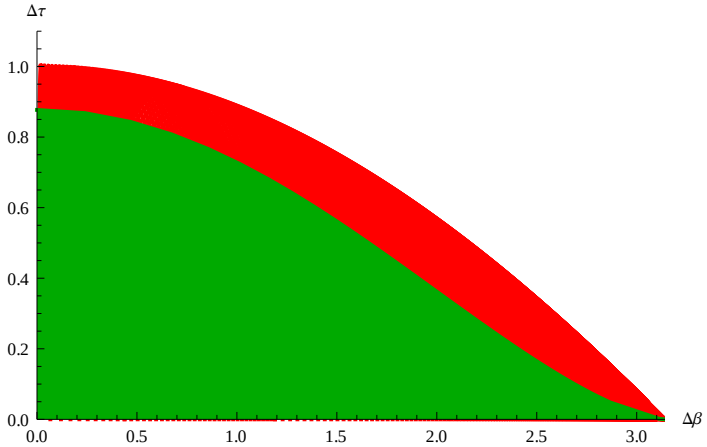

FIGURE 4.7: The phase diagram over $\Delta\beta$ and $\Delta\tau$: again for small separations the connected solution dominates, while increasing both the angular distance or the ratio of the radii the area increases until a phase transition occurs and the disconnected solution starts to dominate.

different phases.

In one phase, when the loops are close to each other, the dominant contribution to the correlator at strong coupling is given by a connected surface, that is a single string stretching between the two fibers. In this phase the expectation value of the correlator depends on the relative positions of the two fibers, on their relative radii and on their couplings with the scalar field.

Taking the fibers apart from each other, either by increasing their angular separation or the ratio of their radii, the system undergoes a first order phase transition. In the new phase, the dominant contribution is given by two disconnected surfaces, each one ending on one of the fibers. The two fibers do not interact anymore and the expectation value of the correlator becomes constant.

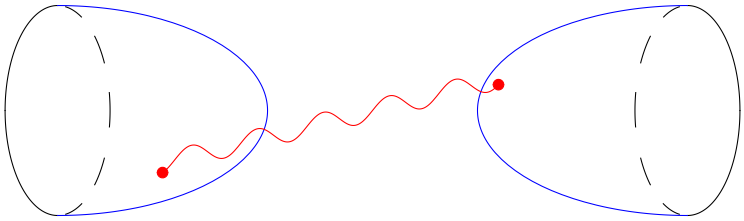

FIGURE 4.8: The exchange of a gravity mode (red line) between the two surfaces of a disconnected classical solution for the correlator of two Wilson loops. The endpoints can sweep the whole worldsheets of each loop.

We expect that this effect should be related to the classical approximation: taking into account the quantum corrections, we should be able to observe a smoothing of the first order transition. The leading correction can be computed in semiclassical approximation as explained in 3.4.

For the case of two disconnected solutions, another kind of corrections must be taken into account. Besides quantum excitations on the classical solution, we must consider the contribution coming from the propagation of gravity modes between the worldsheets of the two strings attached to each one of the loops. To do this, we must integrate the bulk-to-bulk propagator over all possible endpoints on the two worldsheets (see figure 4.8).

The gravity bulk-to-bulk propagator can be thought as a degeneration of the string connecting the two loops. Starting from the connected solution, we note that the surface has a "throat" that becomes narrower as we take the loops apart from each other, either by increasing the angular distances or the ratio between their radii. When the string breaking take place, the throat collapses, hence the connected solution disappear. However, the two surfaces still interact through the exchange of gravity modes, that are the remains of the throat of the connected surface.

This picture suggests that the exchange of gravity mode will smooth the phase transition, resulting either in a second order phase transition or, more likely, in a smooth crossover, where the correlator in the disconnected phase is no more constant. Further investigations in this direction are in progress.

4.3. Weak coupling

In this section we compute the perturbative correlator for two loops with the same radius and the same scalar coupling but opposite orientations

$$\langle W(\psi_1)W(\psi_2)\rangle_{\text{connected}}$$

where $\psi_1 = 2t_1$ and $\psi_2 = -2t_2$, $t_1, t_2 \in [0, 2\pi]$.

The propagator between two points on the same fiber is a constant

$$G^{ab}(x_1, x_2) = \frac{g^2\delta^{ab}}{8\pi^2}$$

For two fibers, we can always choose a coordinate system such that they lie at the same φ but with different θ. The propagator connecting the two loops is then

$$G^{ab}(x, y) = \frac{g^2\delta^{ab}}{8\pi^2}\,(f(u) - 1) \qquad f(u) = \frac{2}{1 - \cos u \cos\frac{\Delta\theta}{2}}$$

where $u = t_1 + t_2$.

For the $U(N)$ gauge group generators $\{T_a\}$ we take the following convention

$$[T_a, T_b] = i f_{abc} T_c \qquad a = 0, 1, \ldots, N^2 - 1 \tag{4.23}$$

$$\operatorname{Tr}(T_a T_b) = \frac{\delta_{ab}}{2} \qquad \operatorname{Tr}(T_a) = \sqrt{\frac{N}{2}}\delta_{a0} \tag{4.24}$$

At the first perturbative order, the only contribution is from the single exchange diagram

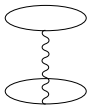

$$= d^{(2)} = \frac{g^2}{8\pi^2}\delta^{ab}\operatorname{Tr}(T_a)\operatorname{Tr}(T_b)\int_0^{2\pi} \mathrm{d}t\,\mathrm{d}s\;(f(u) - 1)$$

The index structure gets summed up as

$$\delta^{ab}\operatorname{Tr}(T_a)\operatorname{Tr}(T_b) = \frac{N}{2}$$

while the integral gives

$$F = \int_0^{2\pi} \mathrm{d}t_1\,\mathrm{d}t_2\;(f(u) - 1) = (2\pi)^2\left(\frac{2}{\sin(\Delta\theta/2)} - 1\right)$$

Finally we get

$$d^{(2)} = \frac{\lambda}{4\pi} T \left(\frac{2}{\sin(\Delta\theta/2)} - 1 \right)$$

where $T = 2\pi$ is the length of the loops.

At order λ^2, there are two inequivalent diagrams:

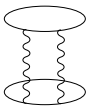

$$= d_1^{(4)} = \left(\frac{g^2}{8\pi^2} \right)^2 \delta^{ac}\delta^{bd} \operatorname{Tr}(T_a T_b) \operatorname{Tr}(T_c T_d) F^2$$

and

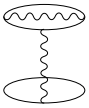

$$= d_2^{(4)} = \left(\frac{g^2}{8\pi^2} \right)^2 \delta^{ac}\delta^{bd} \operatorname{Tr}(T_a T_b T_c) \operatorname{Tr}(T_d) T^2 F$$

Again for the generators we have

$$\delta^{ac}\delta^{bd} \operatorname{Tr}(T_a T_b) \operatorname{Tr}(T_c T_d) = \delta^{ac}\delta^{bd} \operatorname{Tr}(T_a T_b T_c) \operatorname{Tr}(T_d) = \frac{N^2}{4}$$

then

$$d_1^{(4)} = \frac{1}{4} \left(\frac{\lambda}{4\pi} \right) T^2 \left(\frac{2}{\sin(\Delta\theta/2)} - 1 \right)^2$$

$$d_2^{(4)} = \frac{1}{4} \left(\frac{\lambda}{4\pi} \right) T^2 \left(\frac{2}{\sin(\Delta\theta/2)} - 1 \right)$$

It would be important to compute higher order terms, at least up to g^6. As we will see in the next section, this would allow us to compute corrections to the static quark-antiquark potential. However, up to now, it has not been possible to compute the H and X diagram

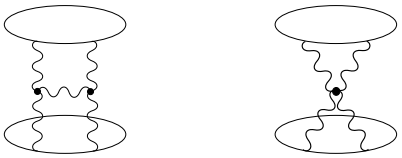

Even in the simpler case, where two circular Wilson loops are involved, these kinds of diagrams are hard to compute and only numerical results are available [46].

4.4. STATIC POTENTIAL

The system of two fibers with opposite orientations with the same scalar charge can be thought as a topologically nontrivial analogue on S^3 of the antiparallel lines describing the static quark-antiquark potential. When the

fibers are sufficiently close to each other, i.e. in the limit $\Delta\theta \to 0$, locally they look like straight lines. In this picture, we expect that the separation distance L between the lines in the static potential

$$V(L) = -\frac{4\pi^2}{\Gamma^4(1/4)}\frac{\sqrt{\lambda}}{L}$$

will be played by the distance between Hopf fibers on the base S^2, which in the S^3 metric is exactly $\Delta\theta/2$. This will indeed be the case.

There's a subtlety in this interpretative picture. While the two antiparallel lines are thought as a degenerate rectangular single loop of infinite extension, involving only one trace, we are dealing with the correlator of two loops, involving two different traces. Nevertheless, our interpretation is still valid, once we take into account both a singlet and an adjoint potential. This is evident if we think to the possible states of a quark-antiquark pair at the same point: the tensor product decomposes onto irreducible representations as

$$\bar{N} \otimes N = 1 \oplus (N^2 - 1) \tag{4.25}$$

The usual strategy to extract the quark-antiquark potential from the Wilson loop is to relate the four point function (in the limit of infinite mass)

$$G(x_1, x_2; y_1, y_2) = \langle 0|T(\bar{Q}(x_1)Q(x_2)Q^\dagger(y_2)\bar{Q}^\dagger(y_1))|0\rangle$$

to the gauge invariant phase experienced by the fields Q's in their temporal evolution, as $T \to 0$. Here $x_{1,2}$ are placed at $T/2$ while $y_{1,2}$ at $-T/2$ (see [47] and [48]).

The field $Q(x)$ has a color index and the general structure of the correlation function in the large T limit, taking $\vec{x}_1 = \vec{y}_1$ and $\vec{x}_2 = \vec{y}_2$ is

$$G(x_1, x_2; t) = \mathbb{P}_S \exp[-TV_S(\vec{x}_1 - \vec{x}_2)] + \mathbb{P}_A \exp[-TV_A(\vec{x}_1 - \vec{x}_2)].$$

where the projectors $\mathbb{P}_S$ and $\mathbb{P}_A$ are defined by the decomposition (4.25).

By taking the relevant traces with the projectors and relating the 4-points functions to correlators of Wilson lines we get

$$\exp[-TV_S(\vec{x}_1 - \vec{x}_2)] = \frac{1}{N}\langle \mathrm{Tr}[W(\vec{x}_1)W^\dagger(\vec{x}_2)]\rangle$$

and

$$\begin{aligned}\exp[-TV_A(\vec{x}_1 - \vec{x}_2)] = \frac{1}{N^2-1}\langle \mathrm{Tr}[W(\vec{x}_1)]\,\mathrm{Tr}[W^\dagger(\vec{x}_2)]\rangle \\ - \frac{1}{N(N^2-1)}\langle \mathrm{Tr}[W(\vec{x}_1)W^\dagger(\vec{x}_2)]\rangle\end{aligned} \tag{4.26}$$

where $W(\vec{x})$ is the Wilson line in $\vec{x}$ extending along the Euclidean time.

The first relation is the usual definition of the quark-antiquark potential V_S in terms of antiparallel Wilson lines.

The second equality gives us a physical interpretation of the correlator of double traced Wilson lines in term of the singlet and adjoint potential V_A.

We can recast it as

$$\frac{N^2-1}{N^2}e^{-TV_A} = W(\vec{x}_1,\vec{x}_2) - \frac{1}{N^2}e^{-TV_S}$$

that expresses the normalized connected correlator $W(\vec{x}_1,\vec{x}_2)$ of the double traced Wilson lines in terms of the potentials. This is the key relation to extract the quark-antiquark potential in the limit of small separation between Hopf fibers from the DGRT loop correlator both at weak and strong coupling.

Assuming for W an expansion in powers of T, $W = \sum_n T^n W_n$, we have up to second order,

$$W_0 = 1 \tag{4.27}$$

$$V_A = -\frac{1}{N^2-1}\left(V_S + N^2 W_1\right) \tag{4.28}$$

$$V_S = -W_1 \pm \sqrt{(N^2-1)(2W_2 - W_1^2)} \tag{4.29}$$

In order to keep track of the powers of N^2 we set

$$\hat{V}_A = N^2 V_A$$
$$\hat{W}_1 = N^2 W_1$$
$$\hat{W}_2 = N^2 W_2$$

so that $\hat{V}_A \sim \hat{W}_1 \sim V_S$ and $\hat{W}_2 \sim V_S^2$ and the (4.29) becomes

$$V_S^2 + \frac{2\hat{W}_1}{N^2}V_S + \frac{\hat{W}_1^2}{N^2} - \frac{2(N^2-1)}{N^2}\hat{W}_2 = 0$$

The solution to this equation in power series of $1/N^2$

$$V_S = -\sqrt{2\hat{W}_2} + \frac{1}{N^2}\left(\frac{\sqrt{2\hat{W}_2}}{2} + \frac{\hat{W}_1^2}{\sqrt{2\hat{W}_2}} - \hat{W}_1\right) + O(N^{-4})$$

In the large N limit we can further expand in powers of g^2

$$V_S = -\sqrt{2W_2^{(2)}}g^2 - \frac{W_2^{(3)}}{\sqrt{2W_2^{(2)}}}g^4.$$

This result shows that if we want to compute the g^4 term of the static potential, we need the g^6 order for the correlator of Wilson loops. However, the computational difficulties in computing Feynman graphs involving a 4-point vertex or two 3-point vertices allows only for numerical computation, as in the case of [46]. We will not attempt this computation and we will only check the leading order result.

At strong coupling, due to the exponentiation property of the Wilson loops correlator, we can directly relate our string solution with the singlet potential. In the $\Delta\theta \to 0$, i.e. $p \to \infty$ limit, the regularized area is

$$A_2^R = \Delta A(p) = A_0\sqrt{p} \tag{4.30}$$

$$A_0 = 4\pi\left(\frac{1}{\sqrt{2}}\,\mathbf{K}(1/2) - \sqrt{2}\,\mathbf{E}(1/2)\right) = -\frac{4\sqrt{2}\pi^{5/2}}{\Gamma(1/4)^2} \tag{4.31}$$

and the angular separation goes as

$$\Delta\theta(p) = \frac{\theta_0}{\sqrt{p}} \tag{4.32}$$

$$\theta_0 = 2\sqrt{2}\,(\,\mathbf{\Pi}(1/2,1/2) - \,\mathbf{K}(1/2)) = \frac{4\sqrt{2}\pi^{3/2}}{\Gamma(1/4)^2} \tag{4.33}$$

hence

$$\sqrt{\lambda}S^R_{\rm min}(p) = \frac{\sqrt{\lambda}}{2\pi}\Delta A(p) = -\frac{16\pi^3}{\Gamma(1/4)^4}.$$

Since

$$\langle WW(A_2^R)\rangle \simeq \exp\left(-\frac{\sqrt{\lambda}}{2\pi}\Delta A(p)\right)$$

we can naturally defined

$$\tilde{V} = -\frac{1}{T}\ln\langle WW(A_2^R)\rangle$$

for $\Delta\theta/T \ll 1$, where $T = 2\pi$ is the length of the fiber in S^3. We find

$$\tilde{V} = -\frac{4\pi^2}{\Gamma(1/4)^4}\frac{\sqrt{\lambda}}{\Delta\theta/2}$$

which coincides with the expected function $V(L)$ once we identify $L = \Delta\theta/2$.

The same result is manifest also at weak coupling, where at the first perturbative order we have

$$\langle W(\psi_{up})W(\psi_{down})\rangle_{\rm conn} = \frac{\lambda}{2}\left(\frac{1}{\sin(\Delta\theta/2)} - 1\right) \simeq \frac{\lambda}{4\pi}\frac{T}{\Delta\theta/2}$$

in agreement with the perturbative calculation for the antiparallel lines

$$\langle W(\psi_{up})W(\psi_{down})\rangle_{\rm conn} = \frac{\lambda}{4\pi}\frac{T}{L}.$$

4.5. HINTS OF 3-POINT FUNCTIONS

One of the most interesting development of this results is the possibility to compute the 3-point correlation functions of a light local operator with two Wilson loops.

The 3-point function $\langle LLL \rangle$ of three light operators, that are operators whose dimensions are independent of the coupling constant, is supersymmetric and is fixed by the symmetry. On the other hand, we can take correlation functions involving also heavy operator, that is operators whose dimension increase with the coupling constant as $\Delta_I \sim \sqrt{\lambda}$.

These objects are not supersymmetric in general. If we take as heavy operator one or more Wilson loops that preserve some supersymmetry, however, we may hope to set up a configuration that is indeed supersymmetric.

Different configurations are possible. If we have only one heavy operator, the correlation function $\langle HLL \rangle$ at strong coupling factorizes [49][50][51]. Each light operator is described by a bulk-to-boundary propagator connecting its position to the insertion point of the corresponding vertex operator on the worldsheet. The leading contribution comes from the diagram where both bulk-to-boundary propagators are attached to the worldsheet, while the diagram with a 3-point interaction in the bulk is subleading.

We are interested in the situation where we have two heavy operators, that are the Wilson loops, and a light local operator. In this case, the correlator $\langle HHL \rangle$ at strong coupling is given by the insertion of the vertex operator on the worldsheet of the string connecting the two loops (when this exists).

This is the first step towards the real missing result, that is the correlation function $\langle HHH \rangle$ of three heavy operators. This kind of correlators have up to now resisted any attempt to compute them, both when involving heavy local operators and Wilson loops. Finding the solution to this problem could enlight new important properties of the theory and we are investigating in this direction.

Chapter 5

Conclusions

In this work we studied the system of two Wilson loops lying on a Hopf fibration on a 3-sphere at the boundary of AdS in the $\mathcal{N} = 4$ SYM theory. We focused on the strong coupling expectation value of this system, that can be computed by the AdS/CFT prescription as the area of the minimal surface extending on the AdS bulk and ending on the Wilson loops at the boundary. Up to now, we only achieved classical results.

The choice of the Hopf fibration was motivated by the interest on supersymmetric systems. Each fiber of the Hopf fibration is a maximal circle on S^3, thus preserving half of the supercharges. The presence of other fibers belonging to the same fibration halves the number of preserved supersymmetries, hence the correlator of two or more equally oriented fibers is 1/4 BPS as a whole.

We found that for non supersymmetric configurations, two different competing solutions are possible. The first one consists of two disconnected surfaces each ending on one of the loops. Each surface is equal to the solution for the single fiber describing the expectation value of a Wilson loop operator.

The second solution describes a single surface stretching in the bulk of AdS between the two loops. The expectation value of the correlator then depends on the relative positions and couplings of the two loops. However, this solution only exists when the two loops are close to each other and the configuration is not supersymmetric because of the wrong relative orientation.

The competition between the two possible solutions gives rise to a phase transition phenomenon. Taking the fibers apart, either increasing the angular separation of the two fibers themselves, the difference between the coupling with the scalar field or the ratio between the radii, the system switches from the connected phase to a disconnected one, through a first order phase transition. The disconnected phase is characterized by the independence of the expectation value of the correlator from the physical quantities describ-

ing the two loops.

This phenomenon was already observed in some particular cases [43][44]. Our result agrees with the literature and we were able to extend the observation of the phase transition to more general configurations.

The phase transition is expected to be smoothed by quantum correction. In particular, taking into account the propagation of gravity modes between the surfaces of the disconnected phase could result in a second order phase transition or, more likely, a smooth crossover.

In some of the configurations considered, the system is supersymmetric. The analysis performed confirms the conjecture [24][25], that supersymmetric Wilson loops are captured by a matrix model. In particular, for the $\mathcal{N} = 4$ theory, the matrix model turns out to be Hermitian and Gaussian and thus it is exactly solvable. Therefore, the result allows to interpolate between weak and strong coupling. The lack of a connected solution for these configurations is a strong argument in favor of the conjecture. However a final proof is still missing, since the non-existence of a connected surface was only proved within an ansatz, which is the most natural but not the most general one.

Strong evidences in support of the conjecture also comes from localization techniques [26].

Many possible developments of this work are at hand.

First of all, it would be interesting to compute the first order quantum corrections to the configurations already considered, in order to analyze the behavior of the phase transition at quantum level. We expect the phase transition to be smoothed and the disconnected phase to receive corrections which depends on the relative position of the loops.

Secondarily, our solutions can be a starting point for the study of 3-point functions involving two Wilson loops and a light local operator. This can be computed by the insertion of the corresponding vertex operator integrated over the worldsheet of the string describing the two Wilson loops correlator. Up to now, the complicated functional dependence of the solution on the parameters prevented the solution of the relevant integral. However, we expect this integral to be solvable at least numerically.

This would be a first step toward the computation of a 3-point function of three heavy operators, which is one of the hottest open problems in this field of research. In the case of three Wilson loops, we should look for smooth minimal surfaces extending in AdS with three different endings on the boundary. This is a highly nontrivial problem in the theory of minimal surfaces.

Finally, in a broader perspective, it would be interesting to extend our results in different target space geometries. We worked in the frame of Euclidean AdS, in order to have a 3-sphere submanifold on the AdS boundary. We can try to generalize the construction to Lorentzian signature. In this case there are no 3-spheres, but we can consider a 3-dimensional hyperbolic

submanifold [52] and try to generalize the Hopf construction. Further, we can consider other gauge theories with AdS gravity dual. A natural candidate in this direction is the $\mathcal{N} = 6$ ABJM theory in three dimensions, which is the maximally supersymmetric theory in three dimensions and whose dual theory at strong coupling is the type IIA superstring on $\mathrm{AdS}_4 \times \mathbb{C}P^3$. Other interesting investigations involve $\mathcal{N} = 2$ and $\mathcal{N} = 2^*$ supersymmetric theories in four dimensions[53]. For these theories a dual gravity theory is not yet known. The analysis of the Wilson loops in this background may yield new results and enlight the string dynamics of the dual theory since the Wilson loop directly couples to the fundamental string worldsheet.

Appendix A

Superalgebra

The algebra of $\mathcal{N}=4$ SYM is $\mathfrak{psu}(2,2|4)$. Its bosonic subalgebra $\mathfrak{so}(2,4) \times \mathfrak{so}(6)$ is the algebra of generator of the isometry group of $\mathrm{AdS}_5 \times S^5$.

We denote the generators of $SU(2)_L \times SU(2)_R$ Lorentz group by $J^{\alpha}{}_{\beta}$ and $\bar{J}^{\dot{\alpha}}{}_{\dot{\beta}}$ and the generators of the R-symmetry group $SU(4)$ by $R^{A}{}_{B}$.

The other bosonic generators are translations $P_{\alpha\dot{\alpha}}$, special conformal transformations $K^{\alpha\dot{\alpha}}$ and the dilaton D.

$$[D, P_{\alpha\dot{\alpha}}] = -iP_{\alpha\dot{\alpha}} \qquad [D, K^{\alpha\dot{\alpha}}] = iK^{\alpha\dot{\alpha}} \tag{A.1}$$

$$\{Q^A_\alpha, \bar{Q}_{B\dot{\alpha}}\} = \delta^A_B P_{\alpha\dot{\alpha}} \qquad \{S^\alpha_A, \bar{S}^{B\dot{\alpha}}\} = \delta^B_A K^{\alpha\dot{\alpha}} \tag{A.2}$$

$$[K^{\alpha\dot{\alpha}}, Q^A_\beta] = \delta^\alpha_\beta \bar{S}^{A\dot{\alpha}} \qquad [K^{\alpha\dot{\alpha}}, \bar{Q}_{A\dot{\beta}}] = \delta^{\dot{\alpha}}_{\dot{\beta}} S^\alpha_A \tag{A.3}$$

$$[P_{\alpha\dot{\alpha}}, S^\beta_A] = -\delta^\beta_\alpha \bar{Q}_{A\dot{\alpha}} \qquad [P_{\alpha\dot{\alpha}}, \bar{S}^{A\dot{\beta}}] = -\delta^{\dot{\beta}}_{\dot{\alpha}} Q^A_t \alpha \tag{A.4}$$

$$\{Q^A_\alpha, S^\beta_B\} = \delta^A_B J^\beta{}_\alpha + \delta^\beta_\alpha R^A{}_B + \frac{1}{2}\delta^A_B \delta^\beta_\alpha D \tag{A.5}$$

$$\{\bar{Q}_{A\dot{\alpha}}, \bar{S}^{B\dot{\beta}}\} = \delta^B_A \bar{J}^{\dot{\beta}}_{\dot{\alpha}} - \delta^{\dot{\beta}}_{\dot{\alpha}} R^B{}_A + \frac{1}{2}\delta^B_A \delta^{\dot{\beta}}_{\dot{\alpha}} D \tag{A.6}$$

$$[K^{\alpha\dot{\alpha}}, P_{\beta\dot{\beta}}] = \delta^{\dot{\alpha}}{}_{\dot{\beta}} J^\alpha{}_\beta + \delta^\alpha_\beta \bar{J}^{\dot{\alpha}}_{\dot{\beta}} + \delta^\alpha_\beta \delta^{\dot{\alpha}}_{\dot{\beta}} D \tag{A.7}$$

Appendix B

Dirac matrices

We want to construct and explicit representation of the 10-dimensional Dirac matrices

$$\{\Gamma^M, \Gamma^N\} = 2\eta^{MN}$$

In $d = 2$ we have the Pauli matrices

$$\tau^1 = \begin{pmatrix} & 1 \\ 1 & \end{pmatrix} \qquad \tau^2 = \begin{pmatrix} & -i \\ i & \end{pmatrix} \qquad \tau^3 = \begin{pmatrix} 1 & \\ & -1 \end{pmatrix} \tag{B.1}$$

which obey to

$$\{\tau^i, \tau^j\} = 2\delta^{ij} \qquad [\tau^i, \tau^j] = i\varepsilon^{ijk}\tau^k \tag{B.2}$$

where $\varepsilon^{123} = 1$.

In $d = 4$ we have the usual representation on the Weyl basis

$$\gamma^0 = \begin{pmatrix} & \mathbb{1} \\ \mathbb{1} & \end{pmatrix} \qquad \gamma^i = \begin{pmatrix} & \tau^i \\ -\tau^i & \end{pmatrix} \tag{B.3}$$

We can build 6-dimensional matrices with Euclidean signature as

$$\Gamma^4 = \sigma^1 \otimes \gamma^0 \qquad \Gamma^{4+j} = i\sigma^3 \otimes \gamma^j \qquad j = 1, 2, 3, \tag{B.4}$$

$$\Gamma^8 = i\sigma^1 \otimes \gamma^5 \qquad \Gamma^9 = \sigma^2 \otimes \mathbb{1}_4 \qquad \bar{\Gamma} = i\sigma^3 \otimes \mathbb{1} \tag{B.5}$$

We can build the 10-dimensional matrices as the tensor product of the ones in 4 and 6 dimension since $2^{10/2} = 2^{6/2} \times 2^{4/2}$. In this way the gamma matrices are already tailored onto the $SO(1,3) \times SO(6)$ subgroup of $SO(1,9$ that is relevant for our theory.

$$\Gamma^\mu = \mathbb{1} \otimes \gamma^\mu \qquad \Gamma^m = \Gamma^m \otimes \bar{\gamma} \tag{B.6}$$

and

$$\bar{\Gamma} = -i\bar{\Gamma} \otimes \gamma^5 = \begin{pmatrix} \mathbb{1}_4 & \\ & -\mathbb{1}_4 \end{pmatrix} \otimes \gamma^5.$$

Appendix C

Elliptic Functions

We follow the conventions of Wolfram functions and Mathematica.

The incomplete elliptic integrals of the first, second and third kind are

$$\mathbf{F}(z|m) = \int_0^z \frac{1}{\sqrt{1-m\sin^2 t}}\mathrm{d}t \tag{C.1}$$

$$= \int_0^{\sin z} \frac{1}{\sqrt{1-t^2}\sqrt{1-mt^2}}\mathrm{d}t \tag{C.2}$$

$$\mathbf{E}(z|m) = \int_0^z \sqrt{1-m\sin^2 t}\mathrm{d}t \tag{C.3}$$

$$= \int_0^{\sin z} \frac{\sqrt{1-mt^2}}{\sqrt{1-t^2}}\mathrm{d}t \tag{C.4}$$

$$\mathbf{\Pi}(n;z|m) = \int_0^z \frac{1}{\left(1-n\sin^2 t\right)\sqrt{1-m\sin^2 t}}\mathrm{d}t \tag{C.5}$$

$$= \int_0^{\sin z} \frac{1}{(1-nt^2)\sqrt{1-t^2}\sqrt{1-mt^2}}\mathrm{d}t \tag{C.6}$$

The corresponding complete integrals are

$$\mathbf{K}(m) = \mathbf{F}(\tfrac{\pi}{2}|m) \tag{C.7}$$

$$\mathbf{E}(m) = \mathbf{E}(\tfrac{\pi}{2}|m) \tag{C.8}$$

$$\mathbf{\Pi}(n|m) = \mathbf{\Pi}(n;\tfrac{\pi}{2}|m) \tag{C.9}$$

Given the integral

$$u = \int_0^{\varphi} \frac{\mathrm{d}\alpha}{\sqrt{1-m\sin^2\alpha}}$$

we define the Jacobi amplitude as

$$\varphi = \mathbf{am}(u|m)$$

The amplitude is an infinitely-many-valued function of u and has period $4i\,\mathbf{K}(m)$.

The sine, cosine and delta amplitude are defined as

$$\begin{aligned}\mathbf{sn}(u,m) &= \sin\,\mathbf{am}(u,m)\\ \mathbf{cn}(u,m) &= \cos\,\mathbf{am}(u,m)\\ \mathbf{dn}(u,m) &= \sqrt{1-m\,\mathbf{sn}^2(u,m)} = \frac{\mathrm{d}}{\mathrm{d}u}\,\mathbf{am}(u|m)\end{aligned}$$

Appendix D

Details of strong coupling correlator

To solve the radial equation

$$R'^2 = \frac{k^2}{4}\left(R^4 + (1-\alpha^2)R^2 - \alpha^2 - t^2 - p^2 - \frac{p^2}{R^2}\right)$$

we have the following integral

$$\frac{k\sigma}{2} = \int_R^\infty \frac{R\,\mathrm{d}R}{\left(R^6 + (1-\alpha^2)R^4 - (\alpha^2 + t^2 + p^2)\,R^2 - p^2\right)^{\frac{1}{2}}}$$

By a change of integration variable $X^2 = \frac{A}{B+R^2}$, we get

$$\frac{k\sqrt{A}\sigma}{2} = \int_0^X \frac{\mathrm{d}X}{\left(1 + \frac{1-\alpha^2-3B}{A}X^2 + \frac{3B^2-2(1-\alpha^2)B-\alpha^2-t^2-p^2}{A^2}X^4\right)^{\frac{1}{2}}}$$

if we require

$$B^3 - (1-\alpha^2)B^2 - (\alpha^2 + t^2 + p^2)B + p^2 = 0. \tag{D.1}$$

For every value of the parameters α, t and p, this equation has three real solutions. We use the following parametrization

$$S_1 = 1 + 3p^2 + 3t^2 + \alpha^2 + \alpha^4 \tag{D.2}$$
$$S_2 = 2 - 18p^2 + 9t^2 + 3\alpha^2 - 9p^2\alpha^2 - 9t^2\alpha^2 - 3\alpha^4 - 2\alpha^6 \tag{D.3}$$
$$Q^2 = 4S_1^3 - S_2^2 \geqslant 0 \tag{D.4}$$

and

$$a_1 = \begin{cases} \arctan \frac{Q}{S_2} & \text{if } S_2 > 0 \\ \frac{\pi}{2} & \text{if } S_2 = 0 \\ \pi + \arctan \frac{Q}{S_2} & \text{if } S_2 < 0 \end{cases} \tag{D.5}$$

$$a_2 = \begin{cases} \pi + \arctan \frac{Q}{S_2} & \text{if } S_2 > 0 \\ \frac{3\pi}{2} & \text{if } S_2 = 0 \\ 2\pi + \arctan \frac{Q}{S_2} & \text{if } S_2 < 0 \end{cases} \tag{D.6}$$

$$a_3 = \begin{cases} \pi - \arctan \frac{Q}{S_2} & \text{if } S_2 > 0 \\ \frac{\pi}{2} & \text{if } S_2 = 0 \\ -\arctan \frac{Q}{S_2} & \text{if } S_2 < 0 \end{cases} \tag{D.7}$$

The solutions to the equation (D.1) are then

$$B_1 = \frac{1}{3}\left((1-\alpha^2) + 2\sqrt{S_2}\cos\frac{a_1}{3}\right) \tag{D.8}$$

$$B_2 = \frac{1}{3}\left((1-\alpha^2) - 2\sqrt{S_2}\cos\frac{a_2}{3}\right) \tag{D.9}$$

$$B_3 = \frac{1}{3}\left((1-\alpha^2) - 2\sqrt{S_2}\cos\frac{a_3}{3}\right) \tag{D.10}$$

We can rewrite the integral as

$$\frac{k\sqrt{A}\sigma}{2} = \int_0^X \frac{\mathrm{d}X}{(1-X^2)^{\frac{1}{2}}(1-lX^2)^{\frac{1}{2}}} = \\ = \mathbf{F}\left(\arcsin X, l\right) \tag{D.11}$$

by fixing

$$A^2 - 2\sqrt{S_1}\cos\frac{a_1}{3}A + \frac{S_1}{3}\left(4\cos^2\frac{a_1}{3} - 1\right) = 0$$

that is

$$A = 2\sqrt{\frac{S_1}{3}}\cos\left(\frac{a_1}{3} - \frac{\pi}{6}\right)$$

and

$$l = \frac{4\cos^2\frac{a_1}{3} - 1}{4\cos^2\left(\frac{a_1}{3} - \frac{\pi}{6}\right)}$$

We can invert (D.11)

$$X = \mathbf{sn}\left(\frac{k\sqrt{A}\sigma}{2}, l\right)$$

then

$$R^2 = \frac{A}{\mathbf{sn}^2\left(\frac{k\sqrt{A}\sigma}{2}, l\right)} - B$$

The range of variation of the worldsheet variable σ is fixed by the point where the surface comes back to the boundary $R \to \infty$

$$\Delta\sigma = \frac{4}{k\sqrt{A}}\,\mathbf{K}(l)$$

The regularized area swept by the surface is then

$$\frac{\text{Area}}{4\pi\sqrt{\lambda}} = \int_R^\infty \mathrm{d}\sigma R^2\Big|_{\text{reg}} = A^{-\frac{1}{2}}\left((A-B)\,\mathbf{K}(l) - A\,\mathbf{E}(l)\right) \tag{D.12}$$

The first integrals (4.9) have solution

$$\begin{aligned}\tau(\sigma) &= \frac{kt}{2}\int_0^\sigma \frac{\mathrm{d}\sigma}{2(1+R^2)} = \\ &= \frac{t}{\sqrt{A}(B-1)}\,\mathbf{\Pi}\left(\frac{B-1}{A}, \mathbf{am}\left(\frac{k\sqrt{A}\sigma}{2}, l\right), l\right) - \frac{k\,t\,\sigma}{2(B-1)}\end{aligned} \tag{D.13}$$

and

$$\begin{aligned}\varphi(\sigma) &= k\,p\int_0^\sigma \frac{\mathrm{d}\sigma}{R^2} = \\ &= \frac{2p}{\sqrt{A}B}\,\mathbf{\Pi}\left(\frac{B}{A}, \mathbf{am}\left(\frac{k\sqrt{A}\sigma}{2}, l\right), l\right) - \frac{k\,p\,\sigma}{B}\end{aligned} \tag{D.14}$$

Evaluating this at $\Delta\sigma$, we find the separation of the fibers (4.16) and the logarithm of the ratio of the radii (4.17).

Bibliography

[1] J. M. Maldacena, *The Large N limit of superconformal field theories and supergravity*, *Adv.Theor.Math.Phys.* **2** (1998) 231–252, [hep-th/9711200].

[2] N. Beisert, C. Ahn, L. F. Alday, Z. Bajnok, J. M. Drummond, et al., *Review of AdS/CFT Integrability: An Overview*, *Lett.Math.Phys.* **99** (2012) 3–32, [arXiv:1012.3982].

[3] E. D'Hoker and D. Z. Freedman, *Supersymmetric gauge theories and the AdS / CFT correspondence*, hep-th/0201253.

[4] G. 't Hooft, *A Planar Diagram Theory for Strong Interactions*, *Nucl.Phys.* **B72** (1974) 461.

[5] R. Metsaev and A. A. Tseytlin, *Type IIB superstring action in AdS(5) x S**5 background*, *Nucl.Phys.* **B533** (1998) 109–126, [hep-th/9805028].

[6] S. Gubser, I. R. Klebanov, and A. M. Polyakov, *Gauge theory correlators from noncritical string theory*, *Phys.Lett.* **B428** (1998) 105–114, [hep-th/9802109].

[7] N. Drukker, S. Giombi, R. Ricci, and D. Trancanelli, *Supersymmetric Wilson loops on S**3*, *JHEP* **0805** (2008) 017, [arXiv:0711.3226].

[8] K. G. Wilson, *Confinement of Quarks*, *Phys.Rev.* **D10** (1974) 2445–2459.

[9] K. Zarembo, *Supersymmetric Wilson loops*, *Nucl.Phys.* **B643** (2002) 157–171, [hep-th/0205160].

[10] D. E. Berenstein, R. Corrado, W. Fischler, and J. M. Maldacena, *The Operator product expansion for Wilson loops and surfaces in the large N limit*, *Phys.Rev.* **D59** (1999) 105023, [hep-th/9809188].

[11] L. F. Alday and A. A. Tseytlin, *On strong-coupling correlation functions of circular Wilson loops and local operators*, *J.Phys.* **A44** (2011) 395401, [arXiv:1105.1537].

[12] J. M. Maldacena, *Wilson loops in large N field theories*, *Phys.Rev.Lett.* **80** (1998) 4859–4862, [hep-th/9803002].

[13] L. F. Alday and J. M. Maldacena, *Gluon scattering amplitudes at strong coupling*, *JHEP* **0706** (2007) 064, [arXiv:0705.0303].

[14] L. F. Alday, J. Maldacena, A. Sever, and P. Vieira, *Y-system for Scattering Amplitudes*, *J.Phys.* **A43** (2010) 485401, [arXiv:1002.2459].

[15] G. Korchemsky, J. Drummond, and E. Sokatchev, *Conformal properties of four-gluon planar amplitudes and Wilson loops*, *Nucl.Phys.* **B795** (2008) 385–408, [arXiv:0707.0243].

[16] J. Drummond, J. Henn, G. Korchemsky, and E. Sokatchev, *Dual superconformal symmetry of scattering amplitudes in N=4 super-Yang-Mills theory*, *Nucl.Phys.* **B828** (2010) 317–374, [arXiv:0807.1095].

[17] D. Correa, J. Henn, J. Maldacena, and A. Sever, *An exact formula for the radiation of a moving quark in N=4 super Yang Mills*, *JHEP* **1206** (2012) 048, [arXiv:1202.4455].

[18] D. Correa, J. Henn, J. Maldacena, and A. Sever, *The cusp anomalous dimension at three loops and beyond*, *JHEP* **1205** (2012) 098, [arXiv:1203.1019].

[19] D. Correa, J. Maldacena, and A. Sever, *The quark anti-quark potential and the cusp anomalous dimension from a TBA equation*, *JHEP* **1208** (2012) 134, [arXiv:1203.1913].

[20] D. Mateos, *String Theory and Quantum Chromodynamics*, *Class.Quant.Grav.* **24** (2007) S713–S740, [arXiv:0709.1523].

[21] G. Policastro, D. Son, and A. Starinets, *The Shear viscosity of strongly coupled N=4 supersymmetric Yang-Mills plasma*, *Phys.Rev.Lett.* **87** (2001) 081601, [hep-th/0104066].

[22] G. T. Horowitz, *Introduction to Holographic Superconductors*, arXiv:1002.1722.

[23] N. Iqbal, H. Liu, and M. Mezei, *Lectures on holographic non-Fermi liquids and quantum phase transitions*, arXiv:1110.3814.

[24] J. Erickson, G. Semenoff, and K. Zarembo, *Wilson loops in N=4 supersymmetric Yang-Mills theory*, *Nucl.Phys.* **B582** (2000) 155–175, [hep-th/0003055].

[25] N. Drukker and D. J. Gross, *An Exact prediction of N=4 SUSYM theory for string theory*, *J.Math.Phys.* **42** (2001) 2896–2914, [hep-th/0010274].

[26] V. Pestun, *Localization of gauge theory on a four-sphere and supersymmetric Wilson loops*, *Commun.Math.Phys.* **313** (2012) 71–129, [arXiv:0712.2824].

[27] M. Marino, *Lectures on localization and matrix models in supersymmetric Chern-Simons-matter theories*, *J.Phys.* **A44** (2011) 463001, [arXiv:1104.0783].

[28] A. Dymarsky, S. S. Gubser, Z. Guralnik, and J. M. Maldacena, *Calibrated surfaces and supersymmetric Wilson loops*, *JHEP* **0609** (2006) 057, [hep-th/0604058].

[29] A. Dymarsky and V. Pestun, *Supersymmetric Wilson loops in N=4 SYM and pure spinors*, *JHEP* **1004** (2010) 115, [arXiv:0911.1841].

[30] S.-J. Rey and J.-T. Yee, *Macroscopic strings as heavy quarks in large N gauge theory and anti-de Sitter supergravity*, *Eur.Phys.J.* **C22** (2001) 379–394, [hep-th/9803001].

[31] N. Drukker, *1/4 BPS circular loops, unstable world-sheet instantons and the matrix model*, *JHEP* **0609** (2006) 004, [hep-th/0605151].

[32] N. Drukker, D. J. Gross, and H. Ooguri, *Wilson loops and minimal surfaces*, *Phys.Rev.* **D60** (1999) 125006, [hep-th/9904191].

[33] N. Drukker and B. Fiol, *On the integrability of Wilson loops in AdS(5) x S**5: Some periodic ansatze*, *JHEP* **0601** (2006) 056, [hep-th/0506058].

[34] N. Drukker, D. J. Gross, and A. A. Tseytlin, *Green-Schwarz string in AdS(5) x S**5: Semiclassical partition function*, *JHEP* **0004** (2000) 021, [hep-th/0001204].

[35] I. Gelfand and A. Yaglom, *Integration in functional spaces and it applications in quantum physics*, *J.Math.Phys.* **1** (1960) 48.

[36] G. V. Dunne, *Functional determinants in quantum field theory*, *J.Phys.* **A41** (2008) 304006, [arXiv:0711.1178].

[37] M. Beccaria, G. Dunne, V. Forini, M. Pawellek, and A. Tseytlin, *Exact computation of one-loop correction to energy of spinning folded string in AdS_5xS^5*, *J.Phys.* **A43** (2010) 165402, [arXiv:1001.4018].

[38] M. Beccaria, G. Dunne, G. Macorini, A. Tirziu, and A. Tseytlin, *Exact computation of one-loop correction to energy of pulsating strings in AdS_5xS^5*, *J.Phys.* **A44** (2011) 015404, [arXiv:1009.2318].

[39] M. Kruczenski and A. Tirziu, *Matching the circular Wilson loop with dual open string solution at 1-loop in strong coupling*, *JHEP* **0805** (2008) 064, [arXiv:0803.0315].

[40] V. Forini, *Quark-antiquark potential in AdS at one loop*, *JHEP* **1011** (2010) 079, [arXiv:1009.3939].

[41] N. Drukker and V. Forini, *Generalized quark-antiquark potential at weak and strong coupling*, *JHEP* **1106** (2011) 131, [arXiv:1105.5144].

[42] L. Griguolo, S. Mori, F. Nieri, and D. Seminara, *Correlators of Hopf Wilson loops in the AdS/CFT correspondence*, *Phys.Rev.* **D86** (2012) 046006, [arXiv:1203.3413].

[43] D. J. Gross and H. Ooguri, *Aspects of large N gauge theory dynamics as seen by string theory*, *Phys.Rev.* **D58** (1998) 106002, [hep-th/9805129].

[44] P. Olesen and K. Zarembo, *Phase transition in Wilson loop correlator from AdS / CFT correspondence*, hep-th/0009210.

[45] S. Giombi, V. Pestun, and R. Ricci, *Notes on supersymmetric Wilson loops on a two-sphere*, *JHEP* **1007** (2010) 088, [arXiv:0905.0665].

[46] J. Plefka and M. Staudacher, *Two loops to two loops in N=4 supersymmetric Yang-Mills theory*, *JHEP* **0109** (2001) 031, [hep-th/0108182].

[47] S. Nadkarni, *Nonabelian Debye screening. 2. The singlet potential*, *Phys.Rev.* **D34** (1986) 3904.

[48] L. S. Brown and W. I. Weisberger, *Remarks on the static potential in quantum chromodynamics*, *Phys.Rev.* **D20** (1979) 3239.

[49] E. Buchbinder and A. Tseytlin, *Semiclassical correlators of three states with large S^5 charges in string theory in AdS_5xS^5*, *Phys.Rev.* **D85** (2012) 026001, [arXiv:1110.5621].

[50] S. Giombi and V. Pestun, *Correlators of Wilson Loops and Local Operators from Multi-Matrix Models and Strings in AdS*, arXiv:1207.7083.

[51] E. Buchbinder and A. Tseytlin, *Correlation function of circular Wilson loop with two local operators and conformal invariance*, arXiv:1208.5138.

[52] V. Branding and N. Drukker, *BPS Wilson loops in N=4 SYM: Examples on hyperbolic submanifolds of space-time*, *Phys.Rev.* **D79** (2009) 106006, [arXiv:0902.4586].

[53] F. Passerini and K. Zarembo, *Wilson Loops in N=2 Super-Yang-Mills from Matrix Model*, *JHEP* **1109** (2011) 102, [arXiv:1106.5763].

List of Figures

1.1 Wilson loop and dual string 11
1.2 Correlation function of a Wilson loop and a local operator . . 13

2.1 Hopf fibration 24

4.1 Area of coincident loops with different scalar couplings 47
4.2 Gross-Ooguri phase transition 48
4.3 Area of loops with same radius and scalar coupling 49
4.4 Area at constant α and p as a function of $\Delta\theta$ and $\Delta\beta$ 52
4.5 Phase diagram of angular separations 53
4.6 Phase diagram on radii ratio and AdS angular separation . . 55
4.7 Phase diagram on radii ratio and S angular separation 55
4.8 Gravity modes exchange between surfaces of disconnected solution. 56

Sì, è lunga, la gratitudine, è come la carità:
non bisogna dimenticare nessuno.
Daniel Pennac - *Grazie*

A tutti quelli che dimenticherò
chiedo venia in anticipo

Al professor Griguolo
per l'aiuto di questi anni

Ai professori Cicuta, Onofri e Bonini
per la disponibilità e i consigli

Ai compagni di viaggio in questo delirio che è il dottorato
in particolare
a "Quelli belli" per la leggerezza
ad Alessio per aver instancabilmente
messo a dura prova la mia pazienza
a Laura per le lamentele trattenute
a Luca per il "genio Toscano"

Agli RdD
(ma non sono sicuro di potervi ancora chiamare così...)
per tutto quello che abbiamo passato
anche dopo anni mi fate sempre sentire a casa

Ai "lettori della Parola"
per le eresie e per le profezie

Ai pellegrini
avete reso speciali questi ultimi mesi.
Spero di continuare a camminare con voi a lungo,
non solo con i piedi

A Mema, Lelo , Becco, Jo,
a Fede e Oliver
non c'è bisogno di dire perché

Alla mia grande famiglia
che mi è sempre stata accanto

A Colui che tutto ha creato
e tutti voi mi ha messo accanto

Grazie!